เซลล์แสงอาทิตย์ชนิดสีย้อมไวแสงที่มี TiO_2 อิเล็กโตรดซึ่งปรับปรุงด้วย La_2O_3, Er_2O_3 หรือ AgO

นายธัญญะ จักรวาฬนรสิงห์

วิทยานิพนธ์นี้เป็นส่วนหนึ่งของการศึกษาตามหลักสูตรปริญญาวิศวกรรมศาสตรมหาบัณฑิต
สาขาวิชาวิศวกรรมเคมี ภาควิชาวิศวกรรมเคมี
คณะวิศวกรรมศาสตร์ จุฬาลงกรณ์มหาวิทยาลัย
ปีการศึกษา 2557

DYE-SENSITIZED SOLAR CELLS WITH TiO_2 ELECTRODE MODIFIED BY La_2O_3, Er_2O_3 or AgO

Mr. Tanya Jakawanorasing

A Thesis Submitted in Partial Fulfillment of the Requirements
for the Degree of Master of Engineering Program in Chemical Engineering
Department of Chemical Engineering
Faculty of Engineering
Chulalongkorn University
Academic Year 2014

Thesis Title	DYE-SENSITIZED SOLAR CELLS WITH TiO_2 ELECTRODE MODIFIED BY La_2O_3, Er_2O_3 or AgO
By	Mr. Tanya Jakawanorasing
Field of Study	Chemical Engineering
Thesis Advisor	Akawat Sirisuk, Ph.D.

Accepted by the Faculty of Engineering, Chulalongkorn University in Partial Fulfillment of the Requirements for the Master's Degree

.....Dean of the Faculty of Engineering

(Professor Bundhit Eua-arporn, Dr.Ing.)

THESIS COMMITTEE

.....Chairman

(Associate Professor Tawatchai Charinpanitkul, Ph.D.)

.....Thesis Advisor

(Akawat Sirisuk, Ph.D.)

.....Examiner

(Palang Bumroongsakulsawat, Ph.D.)

.....External Examiner

(Kanokwan Ngaosuwan, D.Eng.)

ธัญญะ จักรวาฬนรสิงห์ : เซลล์แสงอาทิตย์ชนิดสีย้อมไวแสงที่มี TiO_2 อิเล็กโตรดซึ่งปรับปรุงด้วย La_2O_3, Er_2O_3 หรือ AgO (DYE-SENSITIZED SOLAR CELLS WITH TiO_2 ELECTRODE MODIFIED BY La_2O_3, Er_2O_3 or AgO) อ.ที่ปรึกษาวิทยานิพนธ์หลัก: ดร. อัครวัต ศิริสุข, 65 หน้า.

งานวิจัยนี้มีการปรับปรุงไททาเนียอิเล็กโตรดด้วยการเติมโลหะออกไซด์ ได้แก่ แลนทานัมออกไซด์ เออร์เบียมออกไซด์ หรือซิลเวอร์ออกไซด์ นอกจากนี้ยังศึกษาการเพิ่มชั้นกระเจิงแสงบนอิเล็กโตรดโดยใช้โครงสร้างแบบสองชั้น ซึ่งไททาเนียนั้นเตรียมได้จากวิธีโซล-เจล จากนั้นนำไปเคลือบบนกระจกนำไฟฟ้าเพื่อทำให้เป็นฟิล์มบางด้วยพ่นเครื่องอัลตราโซนิค 500 รอบ แล้วนำไปเผาที่อุณหภูมิ 400 องศาเซลเซียสเป็นเวลาสองชั่วโมง ปริมาณของแลนทานัมออกไซด์ เออร์เบียมออกไซด์และซิลเวอร์ออกไซด์นั้นอยู่ในช่วงร้อยละ 0 ถึงร้อยละ 7 โดยน้ำหนัก หลังจากนั้นนำไปทดสอบหาประสิทธิภาพที่สถาวะมาตรฐาน สำหรับประสิทธิภาพของเซลล์แสงอาทิตย์แบบใช้ไททาเนียเป็นอิเล็กโตรดอยู่ที่ 3.51±0.20% ในกรณีของการเติมแลนทานัมไตรออกไซด์ หรือเออร์เบียมไตรออกไซด์จะทำให้พื้นที่ผิวในการดูดซับสีย้อมมากขึ้นส่งผลให้ค่ากระแสลัดวงจรเพิ่มขึ้น (J_{SC}) ในขณะเดียวกันค่าแรงดันไฟฟ้าขณะเปิดวงจร (V_{OC}) ก็เพิ่มด้วย โดยผลของการเติมแลนทานัมไตรออกไซด์และที่ร้อยละ 5 และการเติมเออร์เบียมไตรออกไซด์ร้อยละ 3 จะเพิ่มประสิทธิภาพเซลล์ถึง 5.06±0.36% และ 4.37±0.30% ตามลำดับ ในทางตรงกันข้ามการเติมซิลเวอร์ออกไซด์นั้นทำให้ประสิทธิภาพของเซลล์ลดลงอย่างมีนัยสำคัญ ส่วนการใช้โครงสร้างแบบสองชั้นพบว่าสามารถช่วยเพิ่มประสิทธิภาพของเซลล์จาก 5.06±0.36% เป็น 7.72±0.47% เมื่อเปรียบเทียบกับอิเล็กโตรดแบบชั้นเดียว โดยการเพิ่มขึ้นของประสิทธิภาพนั้นมาจากผลของการกระเจิงแสงซึ่งช่วยให้แสงนั้นสะท้อนกลับไปยังเซลล์เพิ่มขึ้นนั่นเอง

ภาควิชา วิศวกรรมเคมี ลายมือชื่อนิสิต .....

สาขาวิชา วิศวกรรมเคมี ลายมือชื่อ อ.ที่ปรึกษาหลัก .....

ปีการศึกษา 2557

5670221821 : MAJOR CHEMICAL ENGINEERING

KEYWORDS: DYE-SENSITIZED SOLAR CELL; MIXED OXIDE; SOL-GEL; SPRAY COATING.

TANYA JAKAWANORASING: DYE-SENSITIZED SOLAR CELLS WITH TiO_2 ELECTRODE MODIFIED BY La_2O_3, Er_2O_3 or AgO. ADVISOR: AKAWAT SIRISUK, Ph.D., 65 pp.

In this research, we modified TiO_2 electrode of a dye-sensitized solar cell (DSSC) by adding the second metal oxide, namely lanthanum oxide (La_2O_3), erbium oxide (Er_2O_3) and silver oxide (AgO). Moreover, we also investigated the addition of light scattering layer in the electrode by employing double layered structure. TiO_2-based mixed oxides were synthesized via sol-gel methods. The mixed oxide sols were then coated on a conducting transparent glass as thin film using an ultrasonic spray coater. Finally, the thin film electrode was fired 400°C for 2 h. The amount of La_2O_3, Er_2O_3 or AgO added to TiO_2 was varied from 0 to 7 %wt. The photovoltaic conversion efficiency of pure TiO_2 electrode was 3.51±0.20%, as measured by an IV-tester under standard condition (AM = 1.5). When La_2O_3 or Er_2O_3 was added, the amount of dye adsorbed on the electrode increased due to larger specific surface area of the electrode. As a result, the short circuit current density (J_{sc}) and open circuit voltage (V_{oc}) definitely increased in both cases. The addition of La_2O_3 and Er_2O_3 raised the cell efficiency to 5.06±0.36% with 5 wt% La_2O_3/TiO_2 and 4.37±0.30% with 3 wt% Er_2O_3/TiO_2. On the contrary, the power conversion efficiency was significantly lower with AgO-TiO_2 electrode. Employing the double-layered structure with pure TiO_2 as under-layer and 5%wt La_2O_3/TiO_2 as over-layer enhanced the cell efficiency from 5.06±0.36% to 7.72±0.47% compared to the single-layered La_2O_3-TiO_2 electrode. This can be attributed to light scattering effect, which increased the reflection of light back into the cell.

Department: Chemical Engineering Student's Signature .....

Field of Study: Chemical Engineering Advisor's Signature .....

Academic Year: 2014

ACKNOWLEDGEMENTS

The thesis would not have been possible to succeed without the support of the following individuals. Firstly I wish to express my sincere gratitude to Dr. Akawat Sirisuk, my advisor, for his valuable guidance and enthusiasm throughout the course of my study. And I am also deeply grateful to Associate Professor Tawatchai Charinpanitkul, for his kind supervisor over this thesis as the chairman, Dr. Palang Bumroonsakulsawat and Dr. Kanokwan Ngaosuwan as the members of the thesis committee.

Many thanks for kind suggestions and useful help to staff of NECTEC at NSTDA for solar simulation (IV-tester) and many friends in the Center of Excellence on catalysis and Catalytic Reaction Engineering, who always provide the encouragement and assistance along study. To the many others, not mentioned, who have provided me with support and encouragement, pleased be assured that I always think of you.

Finally, I would like to dedicate this thesis to JAKAWANORASING FAMILY for their infinite support, deeply care throughout my life and listen to my complaints.

CONTENTS

Page

Page

Page

LIST OF TABLES

LIST OF FIGUERS

CHAPTER I
INTRODUCTION

1.1 Rationale

Utilization of fossil fuel gives rise to global warming and environmental pollution. Therefore, we need to replace fossil fuel with renewable energy that is environment friendly for the future. Among the renewable energy, solar energy is an obvious source of environment friendly, clean and cheap energy. Thus harvesting the solar energy with photovoltaic device appears to be a good alternative to solve above problems.

Photovoltaic device (PV) is a device that converts solar energy into electrical power, thereby it has been investigated for a long time in history. First generation of solar cell is the p-n junction of photovoltaic, generally made from mono- and poly-crystalline silicon doped with other elements. These types of solar cell give high power conversion efficiency over 20% [1]; nevertheless, these cells require long fabrication processes that produced some toxicity and consumed a lot of silicon materials. Second generation of solar cell is thin film cells based on amorphous polycrystalline semiconductor compound. In the past, amorphous silicon (A-Si), cadmium telluride (CdTe) and copper indium gallium selenite (CIGS) had been considered as a thin film candidate. But it also required high costs compared to fossil fuel and the efficiency of these cells was lower than wafer-based silicon solar cells that currently dominate the commercial PV market. Third generation of solar cell is still in the research phase that attempted to resolve the problems by increasing the efficiency and decreasing costs such as dye-sensitized solar cells (DSSCs) and polymer solar cell.

DSSCs have been widely studied since firstly reported by O'Regan and Gratzel in 1991 [2]. In terms of low costs, moderate efficiency and simple fabrication, dye-sensitized solar cells (DSSCs) is the promising alternative to conventional silicon solar cells. The DSSCs composed of main five components: a transparent anode

electrode that made out of fluorine-doped tin oxide glass (FTO) with an optimal transparent layer, a mesoporous TiO_2 oxide layer coated on the conducting glass, a dye-sensitizer adsorbed on the TiO_2 layer to enhance light absorption, an electrolyte containing redox mediator and a counter electrode consisting of a glass sheet coated with platinum to facilitate electron collection. The other metal oxide film such as ZnO [3] or SnO_2 [4] have been used as a semiconductor electrode; however, TiO_2 has more stability in various pH, high surface area, compatible with DSSCs and give the highest efficiency conversion compare to the others.

Several attempts have been made to increase the conversion efficiency of solar cells such as modifying the properties of TiO_2 by adding another metal oxide into the lattice of TiO_2 to increase surface area, using pre-coated with passivation layer of another high band gap of metal oxide to prevent the electron recombination, fabricating a double-layered structure as a light scattering layer to boost the light harvesting. Moreover, there have been other approaches to increase the efficiency conversion by developing the dye-sensitizer for absorption in broad wavelength of light or resolving the leakage problems of volatile electrolyte that exhibited remarkable efficiency and stability.

In this research, we focused mainly on the improvement of the power conversion efficiency of DSSC by adding another metal oxide, namely La_2O_3, Er_2O_3 or AgO into lattice of TiO_2 to be used as a thin film electrode layer. The double-layered structure was also investigated to improve on a light scattering of cells and increase light absorption.

1.2 Objectives

1. To enhance the efficiency of a dye-sensitized solar cells with TiO_2 electrode modified by adding La_2O_3, Er_2O_3 and AgO into electrode layer.

2. To improve the efficiency of a dye-sensitized solar cells by using double-layered structure consisting an over- and under-layers film electrode.

1.3 Research scopes

Part I

- Titanium dioxide (TiO_2) and the second metal oxide were prepared by a sol-gel method.
- The amounts of La_2O_3, Er_2O_5 and AgO that were added to TiO_2 ranged from 0 to 10 % (w/w).
- The transparent electrode was characterized by several techniques.
    - X-ray diffraction
    - Nitrogen physisorption
    - UV-visible diffuse reflectance spectroscopy
    - Inductively coupled plasma optical emission spectroscopy
- The efficiency of dye-sensitized solar cell was measured by an IV-tester.

Part II

- Fabricate a DSSC with a double-layered thin film electrode that produced selecting the highest efficiency of metal oxide loading from Part I.
- Characterize the double-layered electrode by several techniques mentioned in part I

This thesis is arranged as follows:

Chapter I presented the introduction and objectives of this study

Chapter II presented the theory of dye-sensitized solar cell including each components and operation principles of dye-sensitizer solar cell (DSSC).

Chapter III presented the literature reviews of previous works related to this research.

Chapter IV presented the synthesis of the TiO_2 sol and modified TiO_2 by a sol-gel methods, preparation of dye-sensitized solar cells, the fabrication procedure and characterization techniques used in this study.

Chapter V presented and discussed the characterization and experimental results.

Chapter VI presented overall conclusion and recommendations for the future studies.

CHAPTER II
THEORY

Dye-sensitized solar cells (DSSC)

Dye-sensitized solar cells have been extensively investigated over long past decades because of ease to fabricated, low production costs and especially cheaper alternative compared to silicon solar cell. The cell is usually based on a titania semiconductor that formed between a working electrode and counter electrode separated by an electrolyte solution. These DSSCs were firstly invented by Michael Gratzel and Brian O'Regan in 1991 and people have also known as Gratzel cells.

2.1 Components of DSSCs

2.1.1 Titanium dioxide (TiO_2) ; Titania

In DSSC, titanium dioxide (TiO_2) is the necessary materials used as thin film semiconductor for DSSC beacause of many reasons. TiO_2 offers appropriate energy levels, the conduction band edge (CB) of TiO_2 places below the excited state energy level of many dyes, which is one condition for efficient electron injection, low cost, and easy preparation [5]. Many researches of DSSCs based on TiO_2 have shown the power conversion efficiency of TiO_2 that was influenced by its crystalline phase, particle size, surface area, dye affinity, and film porosity.

Titanium dioxide presents in three major phases namely anatase, rutile and brookite. The anatase phase have earned a lot of attention among three phases due to its electro-chemical properties, large band gap (Eg = 3.2 eV for anatase), high dielectric constant value (ε = 80 for anatase) and high surface area assuring for dye adsorption. Anatase is metastable and can be easily transformed into more stable phase such a rutile phase when was heating at high temperature. The rutile phase has outstanding light-scattering characteristics due to its high refractive index [6], which is a benificial property of effective light harvesting. However, many literatures have mentioned that the combination of anatase and rutile phase in proper ratio can

express more effective than the pure phase owing to the electron-hole separation at the interface between phases and the formation of interband gap trap which may influence interparticle carrier transportation [5].

There are several methods that can be used to synthesize anatase titania. In general, the method that have been reported for anatase synthesis are a sol-gel method, chemical vapor deposition method, thermal decomposition, and precipitation method [7]. The different method can give the difference of surface area, phase, pore size and morphologies of the titania. Compare to the other techniques, a sol-gel is mostly used because this method has many advantages such as a possibility of making deposited on complex-shaped substrates, easy control of doping level, simple equipment and inexpensive start-up materials [8]. These include that it can be prepared at room temperature, applied by using ultrasonic spray coater to aid dispersion, obtained high surface area and better thermal stability than stirring method.

A sol-gel process occurs in liquid solution of organometallic precursor (e.g. titanium isopropoxide), which lead to the formation of sol by means of hydrolysis and condensation reaction [9].

$$\text{M-O-R} + \text{H}_2\text{O} \rightarrow \text{M-OH} + \text{R-OH} \quad \text{hydrolysis} \quad (2.1)$$

$$\text{M-O-H} + \text{HO-M} \rightarrow \text{M-O-M} + \text{H}_2\text{O} \quad \text{water condensation} \quad (2.2)$$

$$\text{M-O-R} + \text{HO-M} \rightarrow \text{M-O-M} + \text{R-OH} \quad \text{alcohol condensation} \quad (2.3)$$

A typical example of a sol-gel method is addition of metal alkoxide to water. The alkoxide is hydrolyzed, giving the oxide as colloidal product.

The sol is made of many solid particles of few hundred nanometers suspended in a liquid phase. After that, the particles condense into gel, in which solid macromolecules are immersed in a liquid phase. Drying the gel at low

temperature produces porous solid matrices or xerogels. To obtain a final product, the gel is heated. This treatment serves several purposes, i.e. to remove solvent, to decompose anions such as alkoxides or carbonates to give oxides, to rearrange of the structure of solid, and to allow crystallization to occur.

2.1.2 Counter electrode (CE)

The main task of the counter electrode in DSSC is to use as a mediator in regenerating the sensitizer, collecting electrons from external cell after electron injection process, or collection of the holes from the hole conducting material in a DSSC process. The special properties of excellent counter electrode are having high conductance value, a lot of active surface area and good catalyst. So far, many different kinds of counter electrodes have been employed, for example: platinum transparent CE, carbon CE, and conductive polymer CE like PEDOT or polypyrrole. The counter electrode is selected according to the unique application. For power-producing windows or metal-foil-supported DSSCs, one must employ a transparent counter electrode, e.g. a small amount of platinum deposited on F-doped tin oxide coated glass (FTO-glass). Platinum-loaded conducting glass has already been widely used as the standard for DSSC counter electrodes by sputtering or electrochemical deposition method [10]. The reactions at the CE depend on the type of redox shuttle used to transfer charge between the photoelectrode and the CE. In many cases the iodide–triiodide couple has been employed as the redox mediator [11].

2.1.3 Sensitizing dye

Sensitizing dye performs a substanital role to absorb in broad wavelength of sunlight especially in visible wavelength, numerous researches have focused on how to extend the light absorption of several organic metal complexes and organic dyes. Transition coordination complexes (Ru polypyridyl complexes) are employed as charge-transfer sensitizers. These complexes are also one of the most effective sensitizers because of their high efficiency, excellent chemical stability, favorable photo electrochemical properties, and intense charge transfer absorption in the wide

visible range. The most famous among these complexes include the cis-bis(isothiocyanato)bis(4,40-dicarboxylicacid-2,20-bipyridine)Ru (II) coded as N3 or red dye; tris(isothiocyanato)-2,20,2″-terpyridyl-4,40,4″-tricarbolylate)Ru(II) complex, also referred to as black dye, coded as N749; and di(tetrabutylammo-nium)cis-bis(isothiocyanato)bis(4-carboxylicacid-40-carboxylate-2,20-bipyridine)Ru(II), coded as N719 (Figure 2.1). These complexes represent the most efficient sensitizers because of their intense absorption range from the visible to the near-infrared region [12].

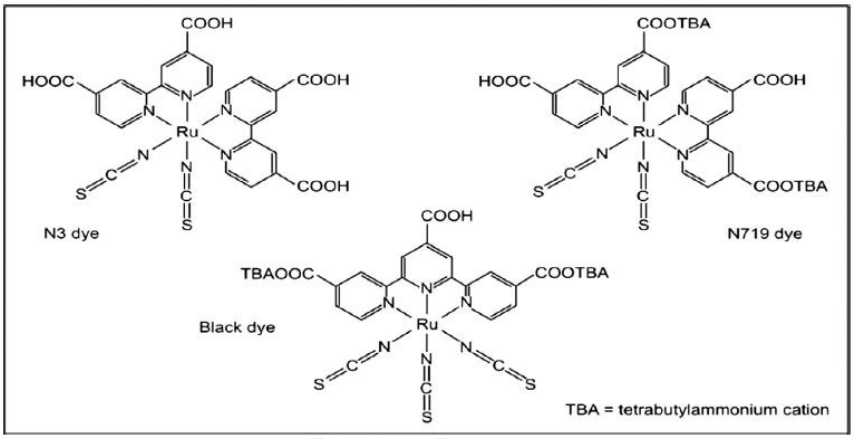

Figure 2.1 Ruthenium metal based organic complexes [13]

The fully protonated N3 has absorption maxima at 518 and 380 nm, the extinction coefficients being 1.3 and 1.33 × 10^4 M^{-1} cm^{-1}, respectively. The complex emits at 750 nm the lifetime being 60 ns. The optical transition has metal-to-ligand charge transfer (MLCT) character: excitation of the dye involves transfer of an electron from the metal to the p* orbital of the surface anchoring carboxylated bipyridyl ligand from where it is released within femto- to picoseconds into the conduction band of TiO_2 generating electric charges with unit quantum yield [14].

Regardless of their chemical stability and the possible exchange of charging with semiconducting solids, Ru complexes have large visible light-harvesting capacity, making them as an excellent choice for the manufacture of solar energy conversion devices.

2.1.4 Electrolyte

The electrolyte is one of an important part of all dye-sensitized solar cells (DSSCs). It operates as charge carriers for collecting electrons at the cathode cell and transfer the electrons back to the dye molecule. The ideal electrolyte would not absorb the visible light and have a good ability to easily occur in redox reaction for compensating the electrons to the excited dye without formation any new chemical compound in the cell. The widespread electrolyte using in DSSC is the iodide/triiodide (I/I_3) redox couple in an organic matrix, typically acetonitrile. However there exist undesirable intrinsic properties which are inherent of a liquid electrolyte significantly affecting a device's long-term durability and operational stability. For example, not only the leakage of toxic organic solvent will cause environmental contamination, but also the evaporation of volatile iodine ions will increase the overall internal resistance by lowering concentration of the charge carrier.

On the other hand, the liquid electrolyte, namely iodide/triiodide (I^-/I_3^-), works well mainly due to its kinetics as shown in Figure 2.2 [15]. The electron injection into the TiO_2 conduction band occurs in the femtosecond time range which is much faster than the electron recombination with I_3^-, and the oxidized dye preferably reacts with I^- than combining with the injected electrons. In the electrolyte, the I_3^- diffuses to cathode to harvest electrons and in turn produce I^- which diffuses in the opposite direction towards the TiO_2 electrode to regenerated dye molecules. The diffusion coefficient of I_3^- ions in the porous TiO_2 structure is about 7.6×10^{-6} cm^2/s [16].

It is found that recombination can be suppressed by adding some of additives to the electrolyte such as 4-tert-butylpyridine (4TBP), guanidiumthiocyanate, and methylbenzimida- zole (MBI). These additives can enhance the efficiency and stability, though they do not participate in the fundamental photoelectrochemical processes. The most probable mechanism is that these additives when absorbed by the TiO_2 surface block the reduction sites to keep electron accept or molecules

away from contact. In theory, the maximum voltage generated in DSSCs is determined by the difference between the quasi-Fermi level of the TiO_2 and the redox potential of the electrolyte, about 0.7 V under solar illumination conditions.

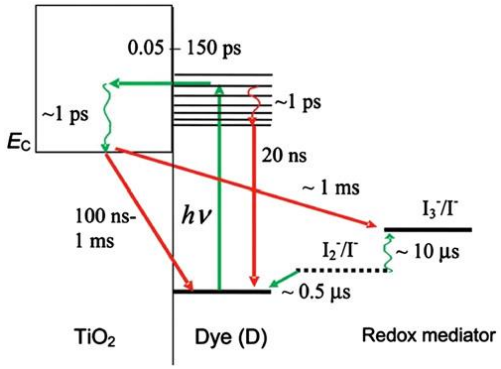

Figure 2.2 Kinetics ofthe cis-$Ru(dcbpy)_2(NCS)_2$-sensitized TiO_2 solar cell with I^-/I_3^- redox mediator [15]

2.2 Operating principles

Operating system of DSSC is different from other kinds of solar cells at all with some noticeable similarities to the natural process of photosynthesis. The operational principle of DSSC is illustrated in Figure 2.3. The first step involves the absorption of photon by the sensitizer S (Eq. (2.4)), which leads to the excitation of the sensitizer S* and the excited sensitizer subsequently injects an electron into the conduction band of the semiconductor, leaving the sensitizer in the oxidized state S^+ (Eq. (2.5)). The injected electron will flow through the semiconductor film to arrive at the back contact and then through the external load to reach the counter electrode in order to reduce the redox mediator (Eq. (2.6)) which in turn regenerates the sensitizer (Eq. (2.7)), completing the circuit [17].

$$S + h\lambda \rightarrow S^*_{(adsorb)} \quad (2.4)$$

$$S^*_{(adsorb)} \rightarrow S^+_{(adsorbed)} + e^-_{injected} \quad (2.5)$$

$$I_3^- + 2e^-_{(cathode)} \rightarrow 3I^- \quad (2.6)$$

$$S^+ + 3/2I^- \rightarrow S + 1/2I_3^- \quad (2.7)$$

Some undesirable reactions including, the recombination of the injected electrons either with oxidized sensitizer (Eq. (2.8)) or with the oxidized redox couple at the semiconductor (TiO_2) surface (Eq. (2.9)) can also occur, resulting in lower cell efficiency.

$$S^{+}_{(adsorbed)} + e^{-}(TiO_2) \rightarrow S_{(adsorbed)} \quad (2.8)$$

$$I_3^{-} + 2e^{-}(TiO_2) \rightarrow 3I^{-}_{(anode)} \quad (2.9)$$

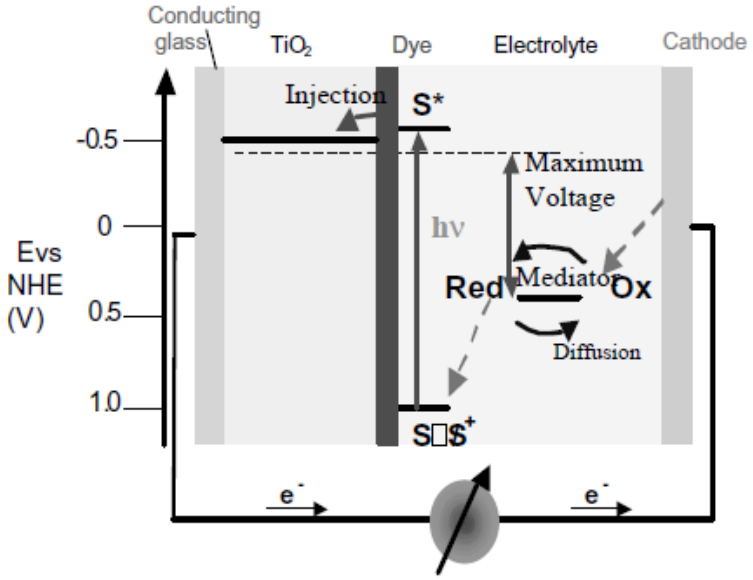

Figure 2.3 Operating principle and energy level diagram of dye-sensitized solar cell [14]

2.3 Characteristic of photovoltaic cell

There are three significant parameters which are used to calculate the power conversion efficiency of DSSC are discussed in the following part such as the short-circuit current (I_{sc}), the open-circuit voltage (V_{oc}) and the fill factor (FF). All of parameters can be computed by using I-V curve.

As its name, I-V characteristic curves show the relationship between the current flowing through an electronic device and the applied voltage across its terminals.

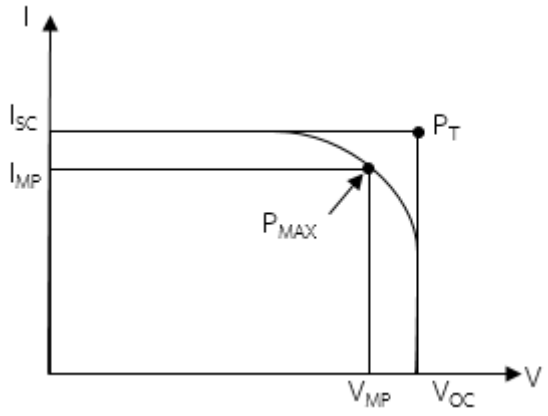

Figure 2.4 IV curve for Photovoltaic cell

2.3.1 Short-circuit current (J_{sc})

Short-circuit current is the electrical current that flows through the solar cell at zero voltage. In order to compare with another cell, it is more common to use the short-circuit current density (J_{SC} in $mA{\cdot}cm^{-2}$) rather than the short-circuit current (I_{SC}) by dividing the area of the solar cell. The short-circuit current is due to the generation and collection of light-generated carriers. Normally, the short-circuit current (I_{SC}) and the light-generated current (I_L) are alike. Therefore, the short-circuit current is the largest current which may be drawn from the solar cell. Likewise, the accurate value of J_{SC} can be determined by integrating the total incident photon to current efficiency (IPCE) and incident photoflux over the spectral distribution.

2.3.2 Open-circuit voltage (V_{oc})

The open-circuit voltage is the maximum voltage available from a solar cell at zero current. The open-circuit voltage corresponds to the amount of forward bias on the solar cell due to the bias of the solar cell junction with the light-generated current. In the band gap theory, the difference between the quasi-Fermi level of

the TiO_2 layer and the electrolyte redox potential determines the maximum voltage generated under illumination.

$$V_{oc} = \frac{kT}{q}\ln(\frac{I_{inj}}{I_{dark}} + 1) \quad (2.12)$$

The above equation shows that V_{oc} relates to the dark current and the injection current. The injection current typically has a small variation whearas the dark current is a key effect to V_{oc}. In fact, dark current is mainly due to the recombination at the TiO_2/dye and TiO_2/electrolyte interface where no photosensitizer got adsorbed. Suppressing of dark current enhances the open circuit voltage of the cell. Hence, open-circuit voltage are used to describe the amount of recombination in the photovoltaic device.

2.3.3 Fill Factor (FF)

The Fill Factor (FF) is essentially a measure of quality of the solar cell. It is calculated by comparing the maximum power to the theoretical power (P_T) that would be output at both the open circuit voltage and short circuit current together. A larger fill factor is desirable, and corresponds to an I-V sweep that is more square-like.

$$\mathrm{FF} = \frac{P_{MAX}}{P_T} = \frac{V_{MP}J_{MP}}{V_{oc}J_{sc}} \quad (2.10)$$

Where P_{MAX} is the maximum power output (W/cm^2),

J_{MP},V_{MP} correspond to maximun current and maximum voltage, respectively.

2.3.4 Efficiency

The overall performance of the solar cell can be evaluated in terms of efficiency (η). Efficiency is the proportion between the electrical power output P_{out} and the solar power input, P_{in} in solar cell. P_{out} can be taken to be P_{MAX} since the solar cell can be operated up to its maximum power output to get the maximum efficiency.

$$\eta = \frac{V_{oc}J_{sc}FF}{P_{in}} \times 100\% \qquad (2.11)$$

Where J_{sc} is the short-circuit current density ($mA \cdot cm^{-2}$),

V_{oc} is the open-circuit voltage (V),

P_{in} is the incident light power ($W \cdot cm^{-2}$),

CHAPTER III
LITERATURE REVIEWS

This chapter presented the literature reviews associated with dye-sensitized solar cell (DSSC).

3.1 Modification of TiO_2 electrode with mixed metal oxide

There are several approaches to improve the performance of solar cells. The most effective approach is modification TiO_2 electrode by adding with the second high band gap metal oxide to change its properties, improve surface area for more dye adsorption or reduce electron recombination rate as follows;

Li and Gu (2012) reported the cell of Er_2O_3-doped-TiO_2 nanoparticle that was prepared by a sol-gel method and coated by blade exhibits much better photovoltaic performance, which is attributed to the doping of Er_2O_3 in theTiO_2 electrode, which increases the speed of excited-state electron injection and decreases there combination of injected electrons. The photoelectrical conversion efficiency is increased from 4.83% to 6.05% under AM 1.5 illumination upon Er_2O_3 doping [18].

Wang et al. (2012) demonstrated the means of enhancing the photovoltaic performance of DSSCs by introducing YOF:(Yb^{3+}, Er^{3+}) into the TiO_2 electrode. By means of up-conversion, YOF: (Yb^{3+}, Er^{3+}) improves light harvesting and the photocurrent. As we knew, Er^{3+} is one of the most efficient rare-earth ions because of its wholesome energy levels in the near infrared region. Besides, as a p-type dopant, YOF:(Yb^{3+}, Er^{3+}) promotes the Fermi energy level of TiO_2 film, thus increasing the photovoltage of the DSSC compared to that of the DSSC without dopant [19].

Yu et al. (2012) modified La_2O_3-TiO_2 nanoporous photoanodes which were fabricated for dye-sensitized solar cells by a dip-coating technic. The formation of coordination bonding between the lanthanide ions and dye molecules enhances the dye adsorption. Moreover, photoelectrochemical characterization results demonstrated that the modified photoanodes possess lower electron transfer resistance than the original TiO_2 photoanodes, which relieve the electron recombination rate. Accordingly, the overall conversion efficiency of the La_2O_3 modified DSSCs was dramatically boosted to 9.67% in comparison with 6.84% of the original DSSCs [20].

Nie et al. (2013) successfully prepared highly ordered vertically oriented La-doped TiO_2 nanotube arrays by a facile electrochemical approach. The electrochemical properties of La-doped TiO_2 nanotube array electrode were studied and the photocurrent was dramatically enhanced. A remarkable and maximum photoconversion efficiency of 0.598% was achieved. It was conclusively shown that the PEC degradation efficiency of PNP on La-doped TiO_2 nanotube arrays electrode was higher than the undoped one [21].

Li et al. (2011) studied silver nanoparticle doped TiO_2 nanofibers, prepared by the electrospinning method. Silver doped TiO_2 was used as the working electrode in dye sensitized solar cells. It was found that the silver nanoparticle doped TiO_2 have a vastly increased photocurrent density resulting in a 25% improved conversion efficiency compared to undoped ones. The increasing performance is classified in two factors: (i) the increased light harvesting efficiency due to the plasmon enhanced optical absorption induced by Ag nanoparticles, and (ii) the improved electron collection efficiency as a result of faster electron transport in the Ag doped TiO_2 nanofiber photoanode [22].

3.2 The structure of TiO_2 electrode of dye-sensitized solar cells

Hwang et al. (2015) investigated the influences of dye-concentration for scattering layer in a dye-sensitized solar cell (DSSC), which is consisted with N719 dye on a bilayer anode with 250 nm-sized TiO_2 film on 20 nm sized TiO_2 film, and compared to a monolayer anode 20 nm-sized TiO_2 film. The photovoltaic conversion efficiency (η) of DSSC with the bilayer anode including a light-scattering layer (LSL-DSSC) was enhanced markedly compared to that of the DSSC with normal transparent layer anode (NTL-DSSC). This implies that the light-scattering layer increased the light amount absorbed by dyes. The η was improved more than 80% in low concentration of dye adsorbed on TiO_2, which is caused by the penetrating light up to the scattering layer.

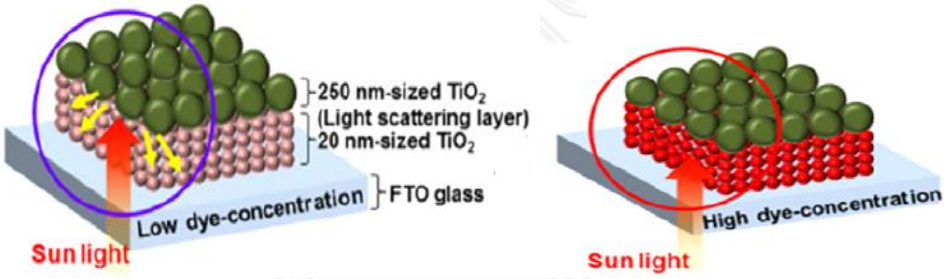

Figure 3.1 Schematics of the scattering layer in a dye-sensitized solar cells consisted with N719 dye on a bilayer anode with 250 nm-sized TiO_2 film on 20 nm sized TiO_2 film, and a monolayer anode 20 nm-sized TiO_2 film [23]

Lee et al. (2009) investigated the improvement of the DSSC performance afforded by using a PEG-based electrolyte and multi-layered TiO_2 electrodes in different type. The application of the light scattering layers resulted in an improvement both the photocurrent flux (J_{sc}) and fill factor, thus increasing the overall power conversion efficiency of the DSSC devices by 64%.

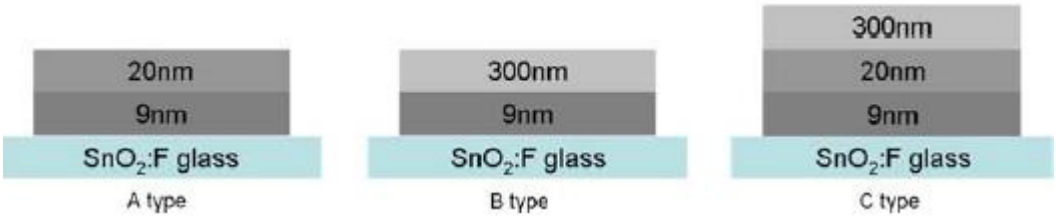

Figure 3.2 Three different types of TiO_2 electrodes on SnO_2:F glass prepared for dye-sensitized solar cells [24]

Chou et al. (2009) investigated the applicability of a hybrid TiO_2 electrode. Most importantly, this study showed that the power conversion efficiency of the DSSC with a hybrid TiO_2 electrode (7.02%), which consisted of 50% TiO_2 particles (P-25) and 50% TiO_2 particles with an average size of 268.7 nm, substantially exceeds that of the conventional DSSC with a TiO_2 (P-25) electrode (5.16%)

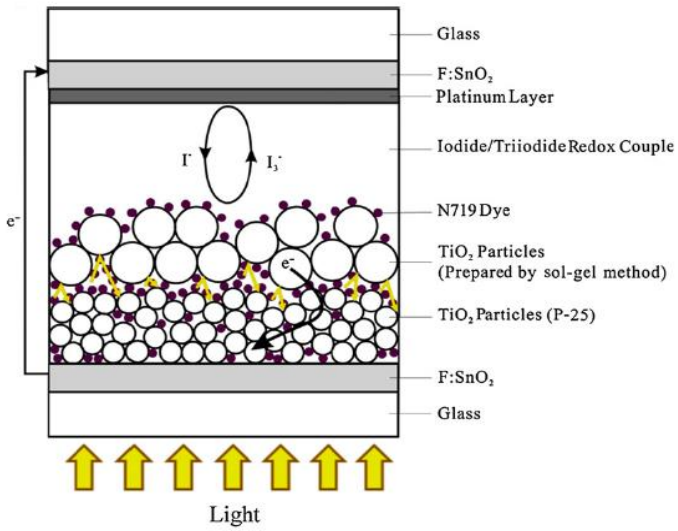

Figure 3.3 Schematics of the DSSC with a layer of TiO_2 particles (P-25) and a layer of TiO_2 particles prepared by the sol–gel method [25]

CHAPTER IV
EXPERIMENTAL

This chapter referred to all materials and methods in this research. The experiments involved in 4 sections: (i) preparation of TiO_2 film and metal oxide doped TiO_2 film. (ii) preparation of dye-sensitized solar cell components. (iii) assembly of DSSC cells in sandwich type by combining working electrode, counter electrode and electrolyte together. (iv) physical and electrochemical characterization.

4.1 Preparation of TiO_2 film and metal oxide doped TiO_2 film

The preparation of TiO_2 film and metal oxide doped TiO_2 flim can be operated by following these two steps. The first step was the preparation of TiO_2 sol via a sol-gel method and the second step was the employment of TiO_2 sol on electrode by ultrasonic spray coating.

4.1.1 Preparation of TiO_2 sol

TiO_2 was synthesized via a sol-gel method by dissolving the starting precursor, titanium isopropoxide (TTIP), in deionized water with 70% nitric acid as a catalyst. The volume ratio between TTIP, deionized water, and nitric acid was 1:12:0.087. After adding TTIP, a white precipitate was instantaneously formed. The mixture was vigorously stirred at least for 3 days until clear sol was obtained and then clean sol was dialyzed in cellulose membrane. The distilled water used for dialysis was changed daily until a pH of sol reached to 3.5. Finally, TiO_2 sol was kept into refrigerator until further used.

4.1.2 Preparation of metal oxide doped TiO_2 sol

In this work, the second metal oxide was added to TiO_2 sol to improve the properties of TiO_2. The precursors of second metal oxide were first dissolved in deionized water. After its pH was adjust to three by using 5M of nitric acid, the

solution was then added into TiO_2 sol according to percent weight in ranging from 0 to 7% (w/w) while being stirred continuously until homogeneous sol was obtained. Finally, the resulting sol was used as spray coater substrates in coating process.

Table 4.1 Preparation of metal oxide doped TiO_2 sol in various percentage

Resulting sol	Precursor	%wt	Volume of Precursor solution (ml)	Volume of TiO_2 sol (ml)
La_2O_3/TiO_2	0.5 g of $La(NO_3)_3{\cdot}6H_2O$ in 50 ml of DI water	1	2.66	47
		3	7.98	46.2
		5	13.3	45.24
		7	18.6	44.29
Er_2O_3/TiO_2	1 g of $Er(NO_3)_3{\cdot}5H_2O$ in 50 ml of DI water	1	1.12	47
		3	3.14	46.2
		5	5.24	45.24
		7	7.34	44.29
AgO/TiO_2	0.5 g of $AgNO_3$ in 50 ml of DI water	1	1.37	47
		3	4.11	46.2
		5	6.85	45.24
		7	9.59	44.29

4.2 Preparation of dye-sensitized solar cell components

DSSCs components consisted of 4 main parts, including transparent conducting oxide glass (TCO), dye, electrolyte, counter electrode and anode electrode or working electrode.

4.2.1 Transparent conducting oxide glass

The transparent conductive oxide glasses, used as an electrode support, was the fluorine doped tin oxide (FTO) glass. The FTO coated glasses demonstrated excellent electrical and optical properties and provided optimal adhesion of coated

layers. The glasses were purchased from Solaronix (Switzerland) under commercial name TCO22-15, which was 2 mm thick glass substrate with a 15 ohm/sq FTO coating at one side. Before use, the glass was cleaned by sonication in detergent solution, acetone and ethanol for 15 minutes in each step and dried with a blow-dryer.

4.2.2 Sensitizing dye

The ruthenium dyes are especially suited for the sensitization of titania. However, cis-diisothiocyanato-bis(2,2'-bipyridyl-4,4'-dicarboxylic acid) ruthenium(II), also known as N3 in literature, was adopted in this research because of its high performance that was active long range of wavelength. The N3 dye was purchased from Solaronix. To prepare the dye solution, 20 mg of N3 dye was dissolved in 100 ml of ethanol and the mixture was sonicated until a homogeneous solution was obtained. The resulting product was a dark purple solution of 0.3 mM N3 dye in ethanol.

4.2.3 Electrolyte

The electrolyte solution was the mixture of 0.5 M lithium iodide (LiI), 0.05 M iodine (I_2) and 0.5 M 4-tert-butylpyridine (4-TBP) in acetronitile. To prepare the electrolyte solution, one mixed 2.00 g of LiI, 0.38g of I_2, and 2.20 ml of TBP in 30 ml of acetonitrile (molar ratio LiI:I_2 :TBP = 0.1:0.01:0.1). The solution was stirred until homogeneity was obtained.

4.2.4 Counter electrode

To prepare the counter electrode, FTO glasses was first cut into a rectangular piece that was 2.0 x 2.5 cm^2 in size. Then two small holes (1-mm diameter) was carefully drilled through the FTO glass by stiletto for electrolyte filling. Next, the perforated glass rectangle was cleaned with detergent solution, acetone and ethanol using a sonicator for 15 minutes in each step. After cleaning, the glass was dried with a blow-dryer. Then, masking tape was placed on one side of the glass as seen in Figure 4.1. Fingerprints were wiped off using a tissue wet with ethanol. Finally,

platinum film was deposited on the FTO glass by using ion sputtering (JEOL:JFC-1100E) at 10 mA of ion current for 6 minutes. After sputtering, masking tape was removed.

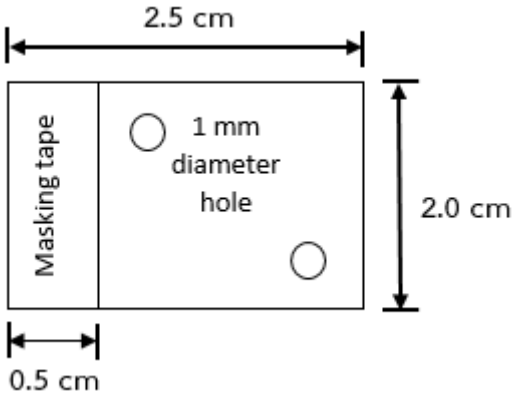

Figure 4.1 The counter electrode before sputtering

4.2.5 Anode electrode or working electrode

As shown in Figure 4.2, to prepare the DSSC working electrodes, the FTO glass used as current collector was first cut to a rectangular piece that was 2.0 x 2.5 cm^2 and then was cleaned in a detergent solution, acetone and ethanol using an ultrasonic bath for 15 min. After cleanup process, the FTO glass was wiped by tissue with wet ethanol for avoid any fingerprints and dried with hair-dryer. Then the glass was masked with aluminum foil that was cut in a circle shape with diameter 0.5 cm as shown in Figure 4.2.

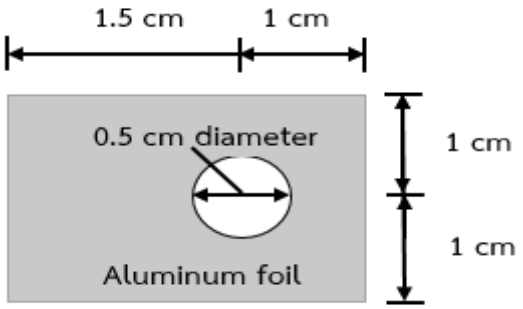

Figure 4.2 The anode electrode before spray coating

After that, TiO_2 was deposited on the conducting glass by using ultrasonic spray coater. Stir the TiO_2 sol before use in coating process, not shake unless bubbles could be formed. TiO_2 sol was placed into a syringe pump, which injected the liquid at a rate 1 ml/min to an ultrasonic nozzle. The level speed of a moving stage was adjusted equal 4. The power of an ultrasonic nozzle that provided by a frequency generator was 3.5-3.6 watts.

In this work, the effect of modified TiO_2 electrode was studied so a number of coats of La_2O_3, Er_2O_3 and AgO was fixed to 500 coats or approximately 10 μm. The thickness of film was measured using profilometer (Veeco Dektak 150). After a few coats, commonly five coats, TiO_2 thin film was dried by hair-dryer. Always make sure that a film strongly packed or completely evaporate before next coats was coming. An anode electrode was sintered at 400°C for two hours and left to be cooled at room temperature. Before dye immersion, an anode electrode was gradually heated to 70°C for 10 minutes to avoid water absorption and then put it slowly into a solution of 0.3 mM N3 dye of 12 hours in the dark. Finally, an anode electrode was rinsed with ethanol (ethanol will remove water from the porous TiO_2) and dried with hair-dryer.

4.3 Assembly of DSSC components

The DSSC was configured in a typical sandwich cell by placing a platinum counter electrode on the top of an anode electrode separated by a 25 μm thick Surlyn film (Solaronix SA, Switzerland). As shown in Figure 4.3, a sealing material was cut in square shape of 2.0x2.0 cm^2 and slashed square hole in the middle.

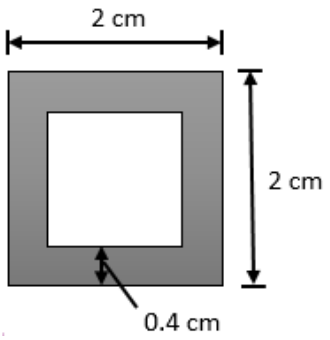

Figure 4.3 The sealing material as a sealant between two electrodes

The two electrodes with sealing sheet were clipped together with 2 clips in the opposite site and heated by hot gun for 3 minutes. A polymer film was melted by heating and glued electrode together. For electrolyte adding, the filling is completely done by putting a droplet on a hole and let it soak up (see Figure 4.4).

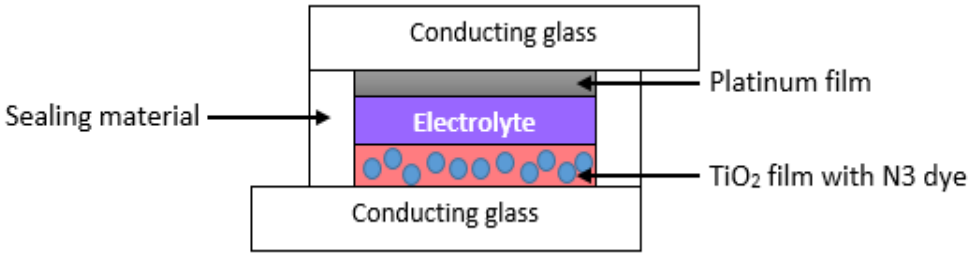

Figure 4.4 Fabrication of dye-sensitized solar cell assembly for testing

Finally, two small holes was sealed off by a clear adhesive tape for preventing electrolyte from leaking. The resulting cell is ready to test.

4.4 Physical and electrochemical characterization

Several techniques of characterization have been used in this work including physical and electrochemical properties of TiO_2, metal oxide doped TiO_2 and sensitizing dye.

4.4.1 X-ray diffractometry (XRD)

XRD was performed to determine crystalline phase and crystallite size of TiO_2, La_2O_3/TiO_2, Er_2O_3/TiO_2 and AgO/TiO_2. It was conducted using a SIEMENS D5000 X-ray diffratometer with Cu Kα radiation (λ = 1.54439 Å) with Ni filter. The spectra were scanned at a rate of 0.04 min^{-1} in the 2θ range of 20-80°.

4.4.2 Nitrogen physisorption

To determine the specific area, The powder of TiO_2, La_2O_3/TiO_2, Er_2O_3/TiO_2 and AgO/TiO_2 were measured by using nitrogen gas adsorption in a continuous flow method at liquid nitrogen temperature. A mixture of nitrogen and helium performed a role of carrier gas using Micromeritics Chemisorb 2750 Pulse Chemisorption system

instrument. The sample was thermally treated at 200°C for one hour before measurement.

4.4.3 UV-Visible spectroscopy (UV-Vis)

Amount of dye adsorption can be measured by a spectroscopic method with measuring the concentration of desorbed dye on the titania film into a mixed solution of 0.1M NaOH and ethanol (1:1 in volume fraction). The absorption value was measured by UV-Vis absorption Spectroscopy (Perkin Elmer Lambda 650, λ = 314 nm).

To study the light adsorption behavior of the catalysts, the absorbance spectra of the catalysts in the wavelength range of 200-800 nm were obtained using Perkin Elmer Lambda 650 spectrophotometer. The step size for the scan was 1 nm and the band gap (E_g) of sample was determined by following equation (4.1):

$$E_g = \frac{1240}{\lambda} \quad (4.1)$$

Where E_g is the band gap (eV) of the sample, λ (nm) is the wavelength of the onset of spectrum.

4.4.4 Inductively Couple Plasma-Atomic Emission Spectroscopy (ICP-AES)

The amount of metal deposited on the surface of titanium dioxide (TiO_2) was measured with an Optima 2100 DV spectrometer. A powder of catalyst was digested into solution phase. Firstly, we dissolved 0.05 g of catalyst 7 ml of 97% H_2SO_4 acid (Sigma Aldrich). Next, 2.7 g of $(NH_4)_2SO_4$ was added into solution while being stirred until homogeneous solution was obtained. Then the resulting solution was made up to 50 ml with deionized water. The solution is ready to measure and compare with a calibration curve to obtain an amount of metal loading.

4.4.5 Current-Voltage Tester (IV-Tester)

The electrochemical properties of dye-sensitized solar cell were determined by IV-tester. Current-Voltage measurement were performed using white light source under air mass (AM) 1.5 condition. To determine current density, open circuit voltage, cell resistance, and fill factor. This information was then converted to efficiency of the solar cell. An area of our solar cell was 0.196 cm^2. The equipment used was MV systems Inc., Xenon short ARC (Osram 1000 W/HS).

CHAPTER V
RESULTS AND DISCUSSION

The focus in this chapter is the effect of addition of mixed metal oxide such as La_2O_3, Er_2O_3 or AgO into TiO_2 electrode by varying percent weight. The performance of dye-sensitized solar cells with double-layered electrode is also described.

5.1 Modification of TiO_2 electrode layer by using mixed metal oxide

5.1.1 Modification of TiO_2 electrode layer by addition La_2O_3

Owing to its advantages, TiO_2 electrode has long been used as anode electrode of DSSCs. Many efforts have been dedicated that how to improve the efficiency of cells effectively and affect to the stability of cells at least. One of many techniques is adding the second metal oxide to improve their properties. TiO_2 electrode was prepared by a sol-gel method and modified by adding La_2O_3 into TiO_2 at various percentage of La_2O_3/TiO_2 (i.e. 1.0%wt, 3.0%wt, 5.0%wt and 7.0%wt). The La_2O_3/TiO_2 was coated 500 times on a conducting glass by an ultrasonic spray coater and was then calcined at 400°C for 2 hours. The thickness of all TiO_2 film electrodes was fixed to 10 μm measured by profilometer.

The XRD patterns of pure TiO_2 and various percentages of La_2O_3/TiO_2 were shown in Figure 5.1. The XRD peak at 2θ value of 25.32°, 37.22°, 48.16° and 62.80° were can be identified to be the anatase phase, whereas The XRD peak at 2θ value of 27.44°, 41.28° and 54.36° corresponded to rutile phase and the peak at 2θ = 30.88° can be assigned to brookite phase [26]. It has been reported that a mixture of anatase and rutile TiO_2 usually produced DSSC with higher efficiency than only one crystal phase [5]. However, anatase phase is a dominant phase that leads to higher photocatalytic activity than rutile phase does. X-ray diffraction (XRD) patterns for pure and doped TiO_2 with La_2O_3 were shown in Figure 5.1.

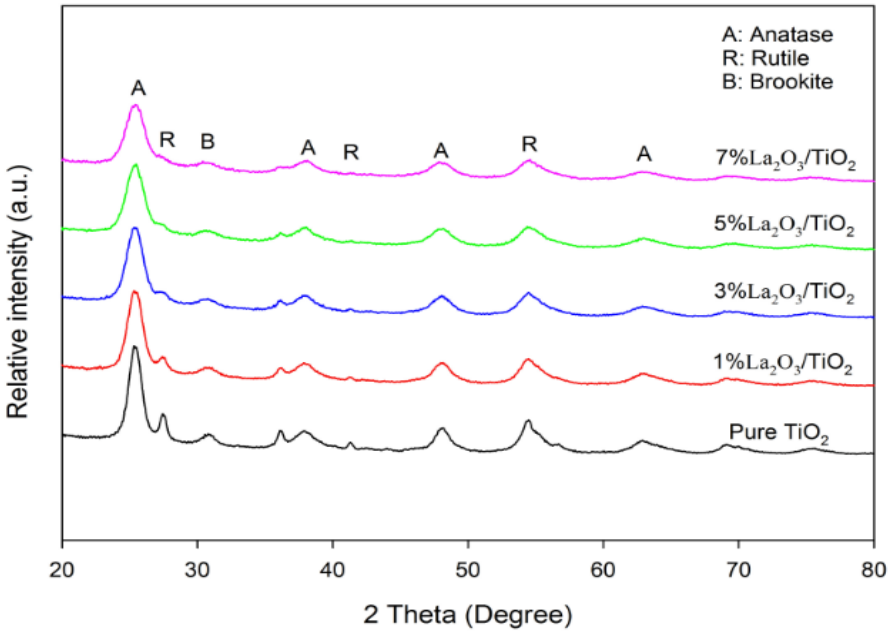

Figure 5.1 XRD patterns of La_2O_3/TiO_2 powders at various percentages

The crystallite size of the samples, calculated using Debye-Scherer formula, were showed in Table 5.1 and the method of titania phase calculation was presented in Appendix B. The size of pure TiO_2 was 7.63 nm and at any higher percentages of La_2O_3/TiO_2, ranging from 1.0%, 3.0, 5.0% and 7.0 %wt presented lower crystallite size than pure TiO_2, respectively. To explain this results, the growth mechanism of pure TiO_2 nanoparticles was involved in the agglomeration of domain structure at the grain boundaries whereas in the case of doped TiO_2 particles, this agglomeration of domain structure is restricted due to the insertion of atomic metal [27]. Furthermore, surface area was measured by single point adsorption using N_2 physisorption method. The specific surface area of La_2O_3/TiO_2 vastly increased compared to pure TiO_2, related to crystallite size. However, specific surface area definitely decreased at 7.0% wt La_2O_3/TiO_2 due to pore blocking or their own surface area of La_2O_3. Weight fraction of TiO_2 was also listed in Table 5.1. All samples are composed of primarily anatase phase and small amounts of rutile and brookite phase.

Moreover, inductively coupled plasma atomic emission spectroscopy was used to confirm the amount of La in Ti catalyst. From Table 5.1, the results assured that La was doped into catalyst but the amount of La is less than expected value. It was probably less than exact value because of the preparation of mixed oxide sol and the error of dilution of ICP standard. The digestion for catalyst powder is also one of difficult problem.

Table 5.1 Crystallite size, surface area and weight fraction of anatase, rutile and brookite of La_2O_3/TiO_2 powder calcined at 400°C for 2 hours

La_2O_3/TiO_2 (w/w)	Crystallite size (nm)	Surface area (m^2/g)	Amount of La_2O_3 from ICP(%wt)	W_A	W_R	W_B
Pure TiO_2	7.6	82	-	0.47	0.21	0.31
1%	7.0	93	0.87	0.48	0.18	0.34
3%	5.8	103	1.87	0.47	0.17	0.36
5%	5.5	110	3.60	0.46	0.17	0.37
7%	5.4	98	5.75	0.43	0.18	0.39

W_A : weight fraction of anatase phase

W_R : weight fraction of rutile phase

W_B : weight fraction of brookite phase

The optical light characteristic was investigated using UV-visible spectroscopy. Table 5.2 showed the wavelength of samples obtained from UV-visible light absorption and the band gap of La_2O_3/TiO_2 in various percentage, whereas Figure 5.2 showed the amount of dye, adsorbed on TiO_2 and La_2O_3/TiO_2 semiconductor. Appendix D presented the example of the calculation of band gap from UV-vis spectra.

In fact, dye sensitized solar cell system required a wide band gap semiconductor that could not be activated over UV range (400 nm) because it will obstruct the absorption of light by N3 dye. The N3 dye is very efficient effective in the visible spectrum up to a wavelength of 750 nm. As we mentioned earlier, we required some doped metal oxide to increase band gap of pure TiO_2. Among the rare earth oxide, La_2O_3 has the largest band gap at 4.3 eV; however, addition of La_2O_3 widened the band gap only slightly (as shown in Table 5.2).

Table 5.2 The comparison band gap from UV-vis spectra of titanium dioxide doped various amount of La_2O_3 calcined at 400°C for 2 hours

Sample	Wavelength (nm)	Band gap energy (eV)
Pure TiO_2	413	3.00
1.0%wt La_2O_3/TiO_2	413	3.00
3.0%wt La_2O_3/TiO_2	407	3.05
5.0%wt La_2O_3/TiO_2	406	3.06
7.0%wt La_2O_3/TiO_2	406	3.06

In addition, we can also figured out the adsorbed dye concentration by dissolving dye from a working electrode with a mixed solution of 0.1 M NaOH and ethanol at a volume ratio 1:1. The dye solution was then analyzed by UV-visible spectrophotometer, using wavelength 314 nm. The amount of dye adsorbed on the surface of TiO_2 and La_2O_3/TiO_2 were showed in Figure 5.2. It was observed that the amounts of dye adsorption with doped La_2O_3/TiO_2 was higher than undoped TiO_2 electrode. The concentration of dye increased when the content of La_2O_3/TiO_2 increased to 5.0% wt and then decreased at 7.0% wt of La_2O_3/TiO_2 that correlated to surface area at Table 5.1. Therefore, it can be concluded that the amounts of adsorbed dye corresponded to surface area of semiconductor.

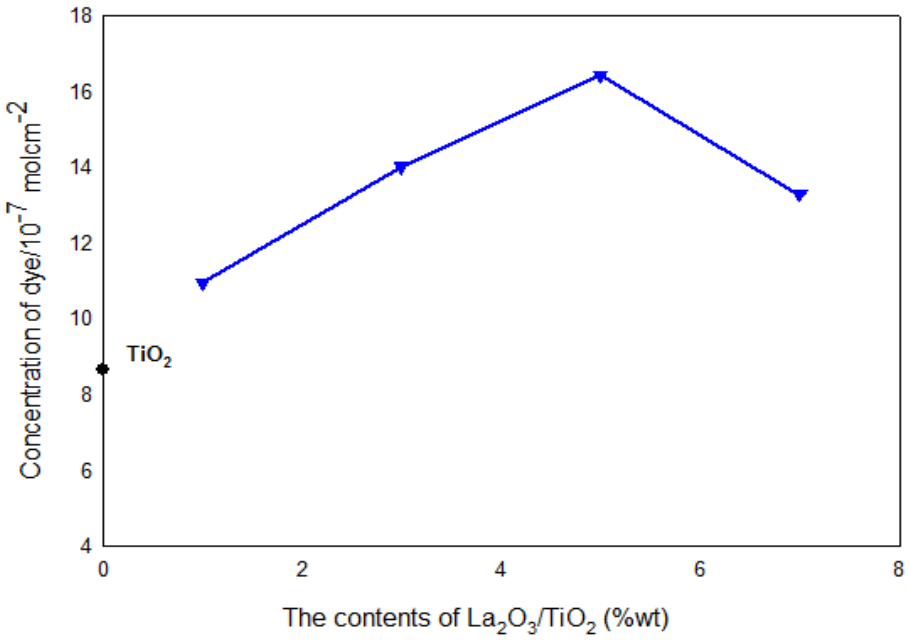

Figure 5.2 Relationship between concentration of dye with various contents of La_2O_3/TiO_2

DSSCs, fabricated using nano-sized particles of TiO_2 and La_2O_3/TiO_2, were prepared by a sol-gel method and coated on FTO glass. A glass was sintered at 400°C for two hours and then immersed into N3 dye. After assembled with counter electrode, all samples have been characterized the electrical properties by measuring the current-voltage (I-V) behavior while irradiating simulated AM 1.5 sunlight with power density of 100 mW/cm^2. Table 5.3 summarized the various parameters calculated from the I-V curve by simulation program. It was clear that higher open circuit voltage (V_{OC}) could be attributed to fewer electron-hole recombination and higher current density (J_{SC}) suggested more electrons that were produced from a light harvest process and injected into conduction band. From the Table 5.3, it was found that the high band gap semiconductor of La_2O_3/TiO_2 acted as an energy barrier at the electrode-electrolyte interface, which decreased the electron-hole recombination rate because of a decrease in open circuit voltage (V_{OC}). Due to a lot of high surface area, the short circuit current density (J_{SC}) of modified electrode also increased too. The efficiency, achieved by DSSC fabricated using La_2O_3/TiO_2, was significantly higher than pure TiO_2 in entire doping level. The highest

efficiency was 5.06±0.36%, obtained from modified TiO_2 electrode by adding 5.0% La_2O_3/TiO_2 and the short circuit current density improved from 6.88 to 7.97 $mA{\cdot}cm^{-2}$ in comparison to pure TiO_2 according to the highest amount of adsorbed dye, specific surface area and band gap.

Table 5.3 Electrochemical properties of dye sensitized solar cell of La_2O_3/TiO_2 electrode calcined at 400°C for 2 hours with 500 coats

La_2O_3/TiO_2 (%wt)	V_{oc} (volt)	J_{sc}($mA{\cdot}cm^{-2}$)	Fill factor	Efficiency (%)
0	0.67	6.88	0.76	3.51±0.20
1.0	0.73	6.83	0.80	3.97±0.19
3.0	0.72	7.30	0.86	4.48±0.39
5.0	0.74	7.97	0.86	5.06±0.36
7.0	0.72	7.38	0.78	4.17±0.63

Note: the efficiency of cells in Table 5.3 is the average value determined from three samples followed by standard derivation.

5.1.2 Modification of TiO_2 electrode layer by addition Er_2O_3

Erbium-doped TiO_2 electrodes for solar cells were prepared via a sol-gel method in various percentage, 1.0%, 3.0%, 5.0% and 7.0% wt. The Er_2O_3/TiO_2 sol was sprayed on the FTO glass substrates 500 times and eventually calcined at 400°C for two hours. Erbium is a one of rare earth and uses of erbium are varied in a lot of applications. In terms of solar cells, it has been investigated not much in literatures or works and the explanation was not clearly as well.

The XRD pattern of TiO_2 and Er_2O_3/TiO_2 were displayed in Figure 5.3. All samples were composed of anatase as a major phase and small amounts of rutile and brookite phase. As seeing that, peak of rutile (2θ=27.44°) decreased when the

concentration of Er_2O_3/TiO_2 increased; however, weight fraction have been calculated thoroughly in number, showing in Table 5.4.

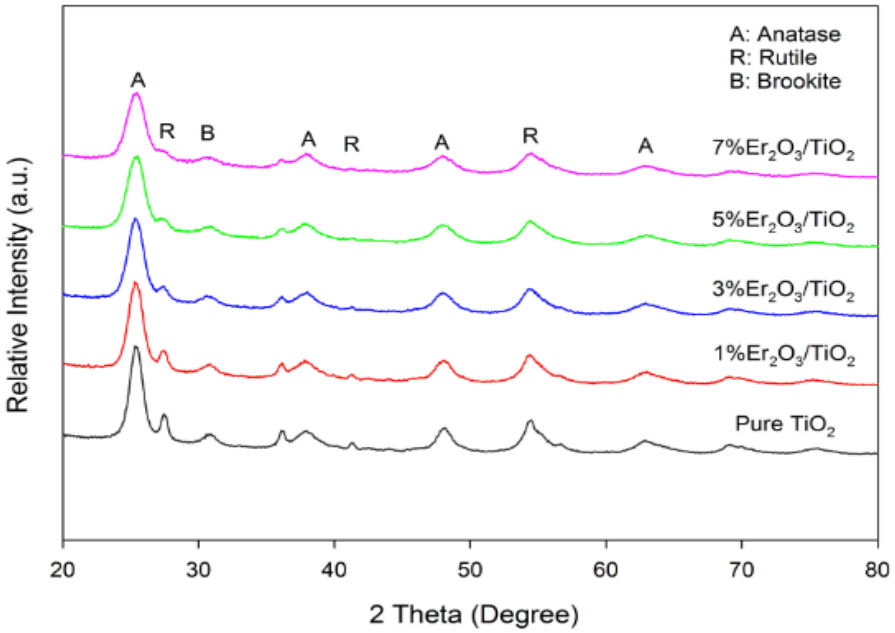

Figure 5.3 XRD patterns of Er_2O_3/TiO_2 powders at various percentages

From Table 5.4, the specific surface area of Er_2O_3/TiO_2, above 1.0% Er_2O_3/TiO_2, was improved compared to pure TiO_2 significantly. The crystallite size of Er_2O_3/TiO_2 decreased when the contents of Er_2O_3/TiO_2 increased. Thus, Er_2O_3 inhibited TiO_2 crystalline growth, leading to small grain size and large specific surface area. The amount of Er was measured by ICP analysis and converted to Er_2O_3/TiO_2 content. ICP results indicated that the content of Er_2O_3/TiO_2 less than intended value in Table 5.4 because of the preparation of mixed oxide sol and the error of dilution of ICP standard. The digestion for catalyst powder is also one of difficult problem.

Table 5.4 Crystallite size, surface area and weight fraction of anatase, rutile and brookite of Er_2O_3/TiO_2 powder calcined at 400°C for 2 hours

Er_2O_3/TiO_2 (w/w)	Crystallite size (nm)	Surface area (m^2/g)	Amount of Er_2O_3 from ICP(%wt)	W_A	W_R	W_B
Pure TiO_2	7.6	82	-	0.47	0.21	0.31
1%	7.1	83	0.84	0.46	0.19	0.35
3%	6.2	96	1.92	0.46	0.18	0.36
5%	6.0	97	3.87	0.44	0.17	0.39
7%	5.8	95	5.95	0.42	0.18	0.40

W_A : weight fraction of anatase phase

W_R : weight fraction of rutile phase

W_B : weight fraction of brookite phase

The band gap energy of mixed oxide was reported in Table 5.5. The intrinsic band gap absorption of TiO_2 was 3.2 eV (388 nm) for anatase phase and 3.0 eV for rutile phase [28]. The band gap of Er_2O_3/TiO_2 was slightly widened to 3.05-3.06 eV above 3.0% wt of Er_2O_3/TiO_2. Even though the absorbed wavelength of Er_2O_3/TiO_2 was higher than 400 nm and blocked light absorption from N3 dye, the band gap of Er_2O_3 doped TiO_2 was fewer than pure TiO_2 at 3.0 eV.

Table 5.5 The comparison band gap from UV-vis spectra of titanium dioxide doped various amount of Er_2O_3 calcined at 400°C for 2 hours

Sample	Wavelength (nm)	Band gap energy (eV)
Pure TiO_2	413	3.00
1.0%wt Er_2O_3/TiO_2	413	3.00
3.0%wt Er_2O_3/TiO_2	406	3.06
5.0%wt Er_2O_3/TiO_2	407	3.05
7.0%wt Er_2O_3/TiO_2	407	3.05

Figure 5.4 displayed the amount of dye adsorbed on TiO_2 electrode. After doping TiO_2 with Er_2O_3, it was obviously clear that all samples can adsorb more dye and affect to boost efficiency by enhanced J_{sc} value. The specific surface area of Er_2O_3/TiO_2 with 3.0%, 5.0% and 7.0% wt was 96, 97 and 95 m^2/g, respectively. However, the highest amount of adsorbed dye contained 3.0% wt Er_2O_3/TiO_2. The decreasing amount of adsorbed dye at 5.0% and 7.0% was obtained because of a poor crystallinity, a fewer specific surface area of Er_2O_3, or a small crystallite size, less than 10 nm, which result in small pores. Thereby, there were a diffused limitation of a molecule of dye and dye affinity [29].

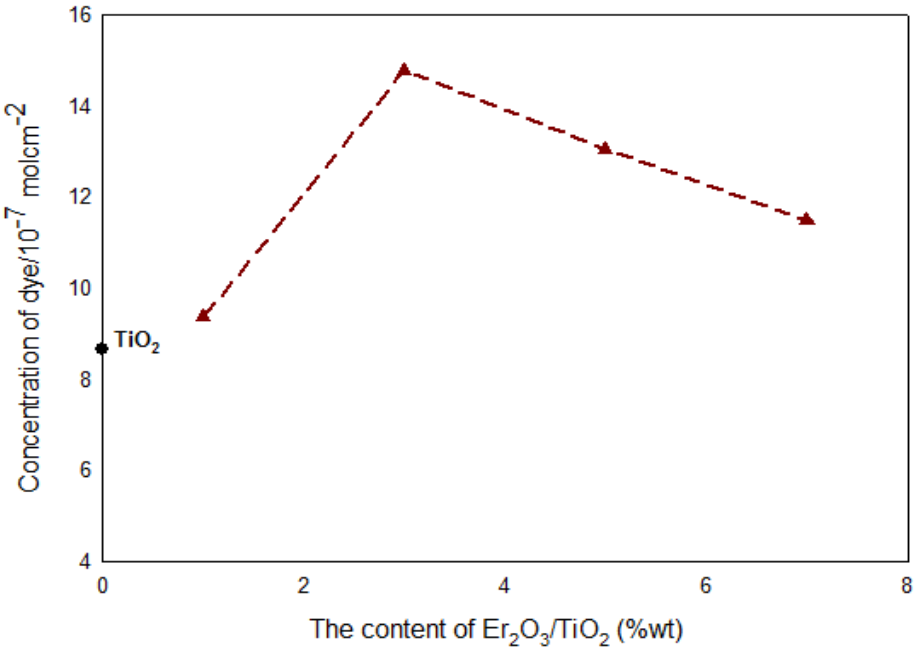

Figure 5.4 Relationship between concentration of dye with various contents of Er_2O_3/TiO_2

The I-V characteristics of DSSC with Er_2O_3/TiO_2 electrode were tabulated in Table 5.6. For pure TiO_2 electrode, the overall cell efficiency was 3.51±0.20%. Modification of TiO_2 electrode with Er_2O_3 raised the conversion efficiency and increased V_{oc}, suggesting that the electron-hole recombination was suppressed. A current density (J_{sc}) also increased because of large specific surface area of modified TiO_2 with Er_2O_3 and a lot of amount of dye adsorbed on TiO_2 surface. Due to the highest amount of adsorbed dye, the highest cell efficiency of 4.37±0.30% was obtained with 3.0% Er_2O_3/TiO_2 electrode.

Table 5.6 Electrochemical properties of dye sensitized solar cell of Er_2O_3/TiO_2 electrode calcined at 400°C for 2 hours with 500 coats

Er_2O_3/TiO_2 (%wt)	V_{oc} (volt)	J_{sc}(mA·cm^{-2})	Fill factor	Efficiency (%)
0	0.67	6.88	0.76	3.51±0.20
1.0	0.71	6.67	0.78	3.69±0.11
3.0	0.75	7.20	0.81	4.37±0.30
5.0	0.72	7.14	0.81	4.17±0.21
7.0	0.72	6.82	0.81	4.01±0.28

Note: the efficiency of cells in Table 5.6 is the average value determined from three samples followed by standard derivation.

5.1.3 Modification of TiO_2 electrode layer by addition AgO

In this section, doped TiO_2 semiconductor were synthesized by adding AgO. The concentration of adding AgO have also been investigated by varied percent of AgO/TiO_2 in several ratio. Modified AgO/TiO_2 sol was prepared by sol-gel method and sprayed on an FTO glass 500 times. The resulting doped TiO_2 electrode was finally fired at 400°C for two hours. From previous in literature review, addition of Ag brought about the effect of surface plasmon that enhanced light absorption by adding Ag ion [22].

XRD patterns of AgO/TiO_2 were shown in Figure 5.5. No peak of AgO was detected and the major phase of all samples was anatase with small amounts of rutile and brookite. No obvious change can be observe by all apparences in any samples. Table 5.7 listed physical properties namely crystallite size, specific surface area and weight fraction of TiO_2 phases in AgO/TiO_2. Unlike La_2O_3/TiO_2 and Er_2O_3, Modification of TiO_2 with AgO decreased specific surface area. Small nano-particles have agglomerated to form grown-up particles, so a large particle size was obtained with increasing AgO contents. The ICP-OES results of silver revealed that silver was presented in the AgO/TiO_2 catalyst. The amount of AgO/TiO_2 were close to the exact

value. The discrepancy was a result of the preparation of mixed oxide sol or digestion for ICP analysis.

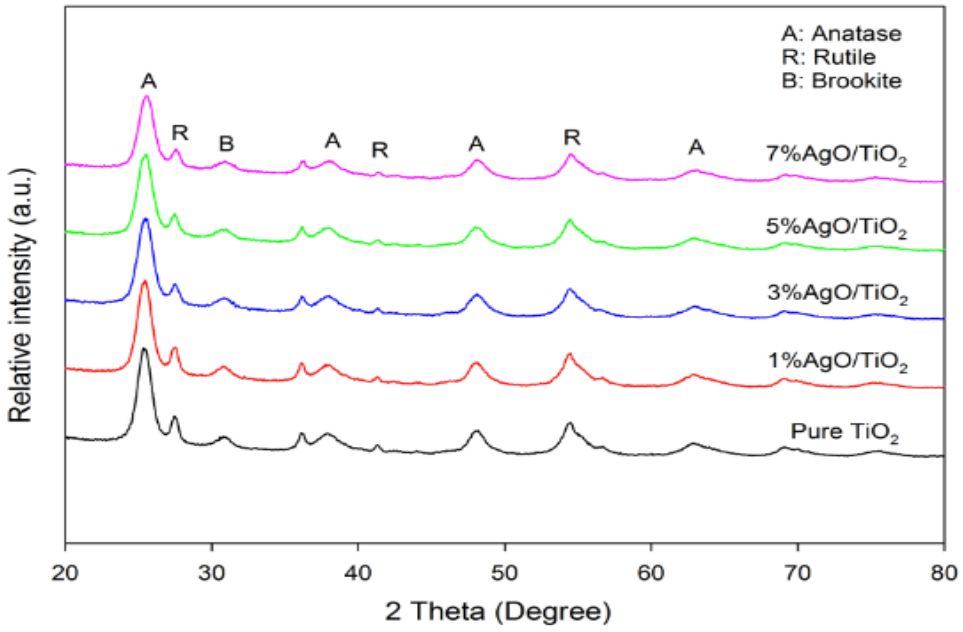

Figure 5.5 XRD patterns of AgO/TiO_2 powders at various percentages

Table 5.7 Crystallite size, surface area and weight fraction of anatase, rutile and brookite of AgO/TiO_2 powder calcined at 400°C for 2 hours

AgO/TiO_2 (w/w)	Crystallite size (nm)	Surface area (m^2/g)	Amount of AgO from ICP(%wt)	W_A	W_R	W_B
Pure TiO_2	7.6	82	-	0.47	0.21	0.31
1%	7.8	82	0.50	0.46	0.21	0.33
3%	8.1	79	2.94	0.45	0.20	0.35
5%	8.7	77	5.77	0.44	0.20	0.36
7%	9.0	71	7.10	0.42	0.20	0.38

W_A : weight fraction of anatase phase

W_R : weight fraction of rutile phase

W_B : weight fraction of brookite phase

Increasing AgO/TiO_2 content lowered the band gap energy of TiO_2 slightly (see Table 5.8). In case of DSSC, band gap under 3.1 eV or absorption wavelength over 400 nm was not suitable because it may block dye absorption wavelength that effective in visible light. In contrast to pure TiO_2, the amount of dye adsorbed on modified TiO_2 electrode drastically decreased (see Figure 5.6) because of lower specific surface area.

Table 5.8 The comparison band gap from UV-vis spectra of titanium dioxide doped various amount of AgO calcined at 400°C for 2 hours

Sample	Wavelength (nm)	Band gap energy (eV)
Pure TiO_2	413	3.00
1.0%wt AgO/TiO_2	420	2.95
3.0%wt AgO/TiO_2	422	2.94
5.0%wt AgO/TiO_2	430	2.89
7.0%wt AgO/TiO_2	432	2.87

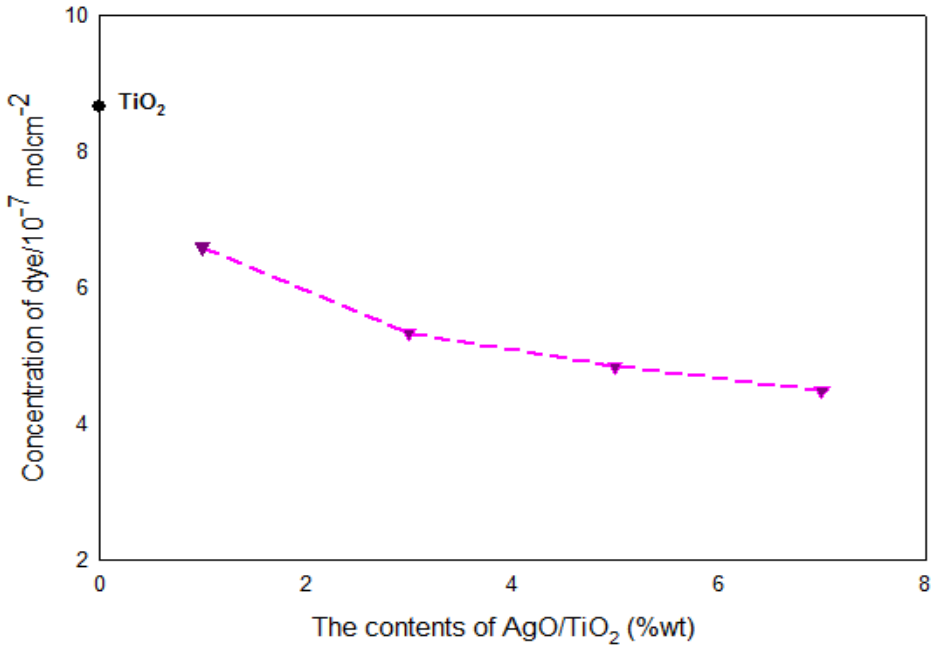

Figure 5.6 Relationship between concentration of dye with various contents of AgO/TiO_2

As per above characterization, the results have shown that doping Ag into TiO_2 was impractical; however, the electrochemical properties were examined. All prepared cells were tested by IV-tester under air mass (AM) 1.5 condition. An area of our solar cell was equal to 0.196 cm^2. Table 5.9 was obtained after determined from IV-curve and three cells were average for one efficiency value. Short-circuit current density was rapidly decreased from 6.88 $mA.cm^{-2}$ for pure TiO_2 to 0.61 $mA.cm^{-2}$ for 7.0% wt AgO/TiO_2. This can be attributed to small specific surface area and partial screening of light from the dye by AgO/TiO_2 layer, Moreover, electrons cannot travel through grain boundaries smoothly. The efficiency of AgO/TiO_2 was drastically decreased from 3.51±0.20% for pure TiO_2 to 0.22±0.04% for 7.0% wt of AgO/TiO_2. Therefore, TiO_2 electrode modified by AgO should not be used in DSSC.

Table 5.9 Electrochemical properties of dye sensitized solar cell of AgO/TiO_2 electrode calcined at 400°C for 2 hours with 500 coats

AgO/TiO_2 (%wt)	V_{oc} (volt)	J_{sc}($mA{\cdot}cm^{-2}$)	Fill factor	Efficiency (%)
0	0.67	6.88	0.76	3.51±0.20
1.0	0.64	5.48	0.70	2.44±0.08
3.0	0.68	3.80	0.64	1.64±0.18
5.0	0.61	2.03	0.63	0.78±0.14
7.0	0.60	0.61	0.59	0.22±0.04

Note: the efficiency of cells in Table 5.9 is the average value determined from three samples followed by standard derivation.

5.2 Modification of dye-sensitized solar cells using double-layered structure

A double-layered structured film with TiO_2 nanoparticles is one type of DSSC structure. It was supposed that double-layered TiO_2 film could markedly improve the efficiency of dye-sensitized solar cells (DSSCs) owing to light scattering effect. Thereby, we attempted to understand the influence the light scattering effect in DSSCs. In this section, we prepared a DSSC device using TiO_2 nanoparticles prepared by a sol-gel method. A TiO_2 sol was coated on FTO glass and fired at 400°C for two hours. In order to examine light scattering effect, we have employed different two structures as follow these;

Structure A: A single-layer structure was employed by deposition of 5.0% wt La_2O_3/TiO_2 film, which was giving the highest efficiency for DSSC, on FTO glass substrate. The number of coats was 500 times and the sintered temperature was 400°C for two hours.

Structure B: A double-layered structure was employed with pure TiO_2 nanoparticles that coated on FTO 250 times and calcined at 400°C for 2 hours as under-layered film. The over-layered film was deposited on FTO glass coated 250 times by using 5.0% wt La_2O_3/TiO_2 sol and calcined at 400°C for 30 minutes. In order to minimize influence from other factions, specific surface area was fixed at the same value of these two structures.

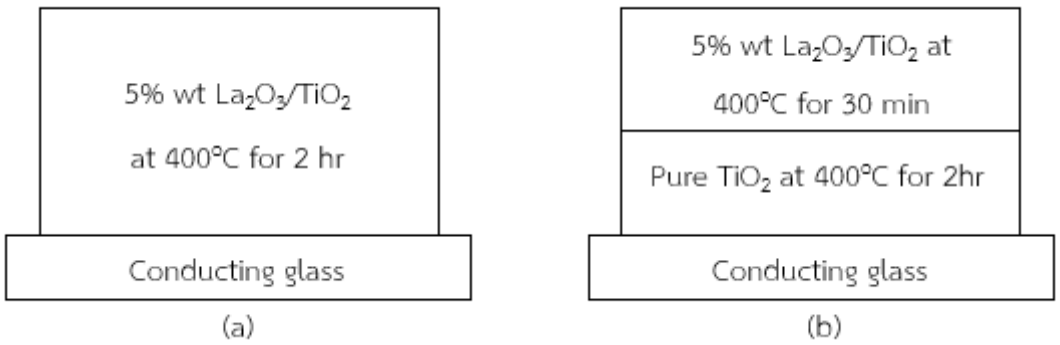

Figure 5.7 Different structures of dye-sensitized solar cell, (a) Single-layer structure (b) Double-layered structure

After that, the electrodes were immersed into N3 dye, anchored on the TiO_2 surface in the dark for 12 hours. The electrodes were then rinsed with ethanol and dried with blower. The physical and chemical properties are measured as same as mention in first part. Table 5.10 presented crystallite size, surface area and concentration of dye adsorption. For single-layered electrode, a mono-particle size was 5.5 nm-La_2O_3/TiO_2 in average diameter. Whereas, double-layered electrode using 5.3 nm-La_2O_3/TiO_2 particles for under-layer and 7.6 nm-TiO_2 particles were also used as over-layer. Light scattering effect appeared from different particle size of two layer. The specific surface area of single-layer structure was 110 m^2/g and the latter structure was (82+117)/2 = 105 m^2/g. The UV-visible spectrophotometer was used for measuring the amount of dye concentration dissolved from porous of semiconductor. The concentration of dye in two structure were close as seen in Table 5.10.

Table 5.10 The properties of single-layer and double-layered structure calcined at various temperatures.

	Sintered Temperature (^oC)	**Crystallite size (nm)**	**Surface area (m^2/g)**	**Concentration of dye ($mol.cm^{-2}$)**
Single-layer: La_2O_3/TiO_2 5.0 wt%	400^{o}C 120 min	5.5	110	16.44×10^{-7}
Double-layer: Pure TiO_2 (under-layer)	400^{o}C 120 min	7.6	82	17.06×10^{-7}
La_2O_3/TiO_2 5.0 wt% (over-layer)	400^{o}C 30 min	5.3	127	

Figure 5.8 compared diffused reflection spectra of two structures. In theory, when incident light projected to samples, most of lights went through a FTO glass and some lights scattered from the glass in different directions. From Figure 5.8, It can implied that double-layered structure has improved diffused reflection since 400 nm up to more than 800 nm compared to single-layer structure. Therefore, it was expected that short-circuit current (J_{sc}) may increase after modification electrode by using double-layered structure.

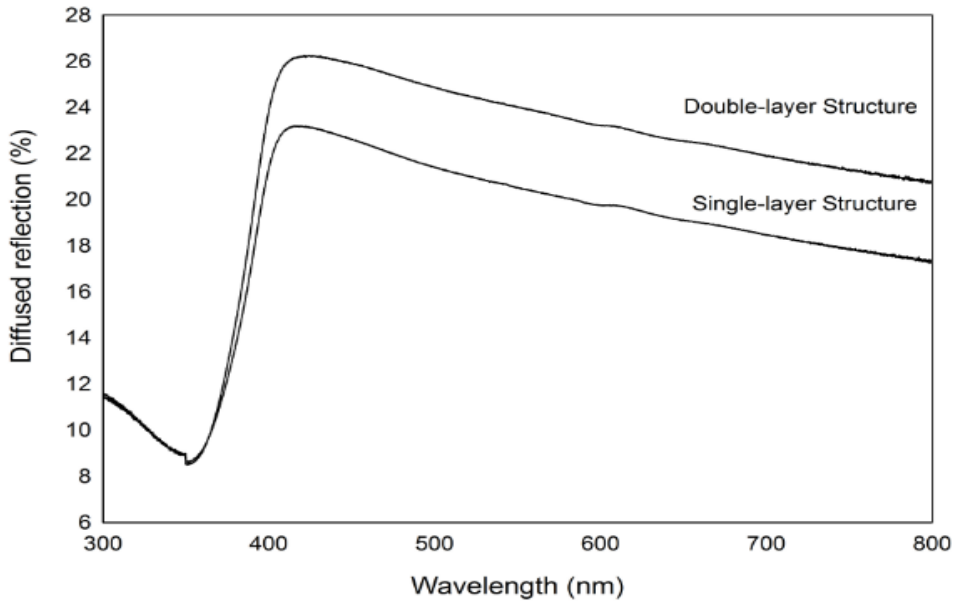

Figure 5.8 Diffused reflection of single-layer and double-layered structure

Table 5.11 showed the electrochemical properties of single-layer and double-layered structure of DSSC that indicated the performance of cells. The photovoltaic properties were measured in same condition as mentioned in above chapter. Short circuit current vastly increased from 7.89 to 13.13 $mA{\cdot}cm^{-2}$ when using of light scattering layer. The decrease of open circuit value is a result of a lower band gap of mixed between pure-TiO_2 and La_2O_3-TiO_2 and more electrons-holes recombination from scattering light effect. The efficiency surprisingly enhanced from 5.06±0.37% for single-layered structure to 7.72±0.47% for double-layered structure.

Table 5.11 DSSC performance of single-layered and double-layered electrode

Structure	V_{oc} (volt)	J_{sc} ($mA \cdot cm^{-2}$)	Fill factor	Efficiency (%)
Single-layer: La_2O_3/TiO_2 5.0 wt%	0.74	7.89	0.87	5.06±0.37
Double-layer: - Pure TiO_2 (under) - La_2O_3/TiO_2 5.0 wt% (over)	0.70	13.13	0.84	7.72±0.47

Note: the efficiency of cells in Table 5.11 is the average value calculated by using three samples followed by standard derivation

CHAPTER VI
CONCLUSION AND RECOMMENDATIONS FOR FUTURE RESEARCH

In summary, we pay a lot of attentions for improving the working electrode to obtain the high conversion efficiency of DSSC by adding another high band gap oxide. Eventually, some mixed-oxides such as La_2O_3, Er_2O_3 or AgO coating on TiO_2 nanoparticles have been experimented and synthesized by means of a simple sol-gel method. The double-layered structured have been also investigated in this work. Chapter VI is divided in two parts: section 6.1 have summarized the results after modified electrode by second metal oxide including using double-layer structure film. Section 6.2 provided the recommendations for the future study.

6.1 Conclusion

6.1.1 Modification of TiO_2 electrode by adding La_2O_3

The role of adding La_2O_3 in TiO_2 electrode was to prevent the recombination, which depends on the different energy of metal oxide/dye/electrolyte interface by increasing band gap of semiconductor. Another advantage of adding La_2O_3 was increase surface area. It was very important because more dye could attach on semiconductor. A previous reasons lead to obtain high power conversion efficiency by increasing open circuit voltage (V_{oc}) and short circuit current (J_{sc}) value. The highest efficiency was 5.06±0.37% obtained by 5.0% of La_2O_3/TiO_2. It can be concluded that La_2O_3/TiO_2 was a beneficial electrode for dye-sensitized solar cell.

6.1.2 Modification of TiO_2 electrode by adding Er_2O_3

The Advantages of adding Er_2O_3 into TiO_2 lattice structure was enlarging band gap of intrinsic TiO_2. Small increasing band gap value assisted at lowering in chance of electrons-holes recombination. The addition of Er_2O_3 also inhibited the crystallite growth of TiO_2 nanoparticles. Er_2O_3 possess high surface area leading to more amounts of adsorbed dye. In contrast to pure TiO_2, the modification of Er_2O_3/TiO_2 gave rise efficiency from 3.51±0.28% to 4.37±0.29% after modified by 3.0% of Er_2O_3/TiO_2 electrode.

6.1.3 Modification of TiO_2 electrode by adding AgO

The addition of AgO was expected to improve short circuit current value by surface plasmon resonance effect. It seems like to enhance power conversion efficiency; on the contrary, addition of AgO gave an inferior outcome. Unlike La_2O_3 and Er_2O_3, AgO lowered both surface area for adsorbed dye and band gap value. Therefore modification of TiO_2 by adding AgO dropped the power conversion efficiency significantly.

6.1.4 Modification of electrode by employing double-layered structure

Double-layered structure was synthesized by combining two layer electrode at different particles size. These structure promoted the amounts of electron from light scattering effect. The efficiency was heighten from 5.06±0.37% to 7.72±0.47% compared to single-layer of 5.0% La_2O_3/TiO_2 electrode.

6.2 Recommendations for future studies

From the previous conclusions, the following recommendations for future studies are proposed.

1. Improving the individual properties of titania semiconductor with other metal oxide
2. Using another method to prepare titania electrode compared to the conventional sol-gel method
3. Enhancing light scattering effect using different multi-structure electrode

REFERENCES

[1] Jay, F., et al. Advanced process for n-type mono-like silicon a-Si:H/c-Si heterojunction solar cells with 21.5% efficiency. Solar Energy Materials and Solar Cells 130 (2014): 690-695.

[2] O'Regan, B. and Gratzel, M. A low-cost, high-efficiency solar cell based on dye-sensitized colloidal TiO2 films. Nature 353(6346) (1991): 737-740.

[3] Srivastava, P. and Bahadur, L. Dye-sensitized solar cell based on nanocrystalline ZnO thin film electrodes combined with a novel light absorbing dye Coomassie Brilliant Blue in acetonitrile solution. International Journal of Hydrogen Energy 37(6) (2012): 4863-4870.

[4] Lee, J.-H., Park, N.-G., and Shin, Y.-J. Nano-grain SnO_2 electrodes for high conversion efficiency SnO2–DSSC. Solar Energy Materials and Solar Cells 95(1) (2011): 179-183.

[5] Wang, H.-H., et al. Preparation of Nanoporous TiO_2 electrodes for Dye-Sensitized Solar Cells. Journal of Nanomaterials 2011 (2011): 1-7.

[6] Ghanbari Niaki, A.H., Bakhshayesh, A.M., and Mohammadi, M.R. Double-layer dye-sensitized solar cells based on Zn-doped TiO_2 transparent and light scattering layers: Improving electron injection and light scattering effect. Solar Energy 103 (2014): 210-222.

[7] Karthikeyan, C.S., Thelakkat, M., and Willert-Porada, M. Different mesoporous titania films for solid-state dye sensitised solar cells. Thin Solid Films 511-512 (2006): 187-194.

[8] Lee, Y., Chae, J., and Kang, M. Comparison of the photovoltaic efficiency on DSSC for nanometer sized TiO_2 using a conventional sol–gel and solvothermal methods. Journal of Industrial and Engineering Chemistry 16(4) (2010): 609-614.

[9] O. Harizanov1 , A.H. <developement and investigation sol-gel TiO_2.pdf>. Solar Energy Materials & Solar Cells 63 (2000): 185-195.

[10] Quiñones, C., Vallejo, W., and Mesa, F. Physical and electrochemical study of platinum thin films deposited by sputtering and electrochemical methods. Applied Surface Science 257(17) (2011): 7545-7550.

[11] Murakami, T.N. and Grätzel, M. Counter electrodes for DSC: Application of functional materials as catalysts. Inorganica Chimica Acta 361(3) (2008): 572-580.

[12] Ludin, N.A., Al-Alwani Mahmoud, A.M., Bakar Mohamad, A., Kadhum, A.A.H., Sopian, K., and Abdul Karim, N.S. Review on the development of natural dye photosensitizer for dye-sensitized solar cells. Renewable and Sustainable Energy Reviews 31 (2014): 386-396.

[13] Basheer, B., Mathew, D., George, B.K., and Reghunadhan Nair, C.P. An overview on the spectrum of sensitizers: The heart of Dye Sensitized Solar Cells. Solar Energy 108 (2014): 479-507.

[14] Grätzel, M. Dye-sensitized solar cells. Journal of Photochemistry and Photobiology C: Photochemistry Reviews 4(2) (2003): 145-153.

[15] Boschloo G, H.A. Characteristics of the Iodide/Triiodide Redox mediator in Dye-Sensitized Solar Cells. Accounts of Chemical Research 42(11) (2009): 1819-1826.

[16] Gong, J., Liang, J., and Sumathy, K. Review on dye-sensitized solar cells (DSSCs): Fundamental concepts and novel materials. Renewable and Sustainable Energy Reviews 16(8) (2012): 5848-5860.

[17] Nazeeruddin, M.K., Baranoff, E., and Grätzel, M. Dye-sensitized solar cells: A brief overview. Solar Energy 85(6) (2011): 1172-1178.

[18] Li, F. and Gu, Y. Improvement of performance of dye-sensitized solar cells by doping Er_2O_3 into TiO_2 electrodes. Materials Science in Semiconductor Processing 15(1) (2012): 11-14.

[19] Wang, J., et al. Application of Yb^{3+}, Er^{3+}-doped yttrium oxyfluoride nanocrystals in dye-sensitized solar cells. Electrochimica Acta 70 (2012): 131-135.

[20] Yu, H., et al. High-performance nanoporous TiO_2/La_2O_3 hybrid photoanode for dye-sensitized solar cells. ACS Appl Mater Interfaces 4(3) (2012): 1289-94.

[21] Nie, J., Mo, Y., Zheng, B., Yuan, H., and Xiao, D. Electrochemical fabrication of lanthanum-doped TiO_2 nanotube array electrode and investigation of its photoelectrochemical capability. Electrochimica Acta 90 (2013): 589-596.

[22] Li, J., et al. Silver nanoparticle doped TiO_2 nanofiber dye sensitized solar cells. Chemical Physics Letters 514(1-3) (2011): 141-145.

[23] Hwang, K.-J., Park, D.-W., Jin, S., Kang, S.O., and Cho, D.W. Influence of dye-concentration on the light-scattering effect in dye-sensitized solar cell. Materials Chemistry and Physics 149-150 (2015): 594-600.

[24] Lee, J.-K., et al. Multi-layered TiO_2 nanostructured films for dye-sensitized solar cells. Journal of Materials Science: Materials in Electronics 20(S1) (2008): 446-450.

[25] Chou, C.-S., Guo, M.-G., Liu, K.-H., and Chen, Y.-S. Preparation of TiO_2 particles and their applications in the light scattering layer of a dye-sensitized solar cell. Applied Energy 92 (2012): 224-233.

[26] Porkodi, K. and Arokiamary, S.D. Synthesis and spectroscopic characterization of nanostructured anatase titania: A photocatalyst. Materials Characterization 58(6) (2007): 495-503.

[27] Kaur, M. and Verma, N.K. $CaCO_3/TiO_2$ Nanoparticles Based Dye Sensitized Solar Cell. Journal of Materials Science & Technology 30(4) (2014): 328-334.

[28] A. Sclafani, J.M.H. <anatase vs rutile phase.pdf>. Comparison of the Photoelectronic and Photocatalytic Activities of Various Anatase and Rutile Forms of Titania in Pure Liquid Organic Phases and in Aqueous Solutions 100 (1996): 13655-13661.

[29] Andreas Kay, M.G. <gratzel 2005 low cost jawwaw.pdf>. Low cost photovoltaic modules based on dye sensitized nanocrystalline titanium dioxide and carbon powder 44 (1996): 99-117.

[30] Banfield, H.Z.a.J.F. <understanding phase anatase rutile brookite.pdf>. Understanding Polymorphic Phase Transformation Behavior during Growth of Nanocrystalline Aggregates: Insights from TiO_2 104 (2000): 3481-3487.

APPENDICES

APPENDIX A
CALCULATION OF THE CRYSTALLITE SIZE

Calculation of the crystallite size by Debye-Scherrer equation

The crystallite size can be calculated from 2θ profile analysis, FWHM, by Debye-Scherrer equation that was suitable for particle size below 100 nm.

From Scherrer equation :

$$D = \frac{k\lambda}{\beta\cos\theta} \qquad \text{(A.1)}$$

Where D = Crystallite size, Å

K = Crystalline-shape factor = 0.9

λ = X-ray wavelength, 1.5418 Å for Cu$K\alpha$

θ = Observed peak angle, degree

β = X-ray diffraction broadening, radian

The X-ray diffraction broading (β) is the pure width of the powder diffraction, free of all broadening due to the experimental equipment. Standard λ-alumina is used to observe the instrumental broadening since its crystallite size is larger than 2000 Å. The X-ray diffraction broadening (β) can be obtained by using Warren's formula.

From Warren's formula

$$\beta^2 = B_M^2 - B_S^2$$
$$\beta = \sqrt{B_M^2 - B_S^2} \quad \text{(A.2)}$$

Where B_M = Measured peak width in radians at half peak height

B_S = Corresponding width of a standard material

Example : calculation of the crystallite site of TiO_2 calcined at 400°C

The half-weight width of (101) diffraction peak = 1.0602°

= 0.018504 radian

The corresponding half-height width of peak of TiO_2 = 0.003836 radian

The pure width = $\sqrt{B_M^2 - B_S^2}$

= $\sqrt{0.018504^2 - 0.003836^2}$

= 0.0181 radian

β = 0.0181 radian

2θ = 25.3259°

θ = 12.663

λ = 1.5418 Å

The crystallite size = $\frac{0.9 \times 1.5418}{0.0181 cos 12.663}$ = 76.30 Å = 7.63 nm

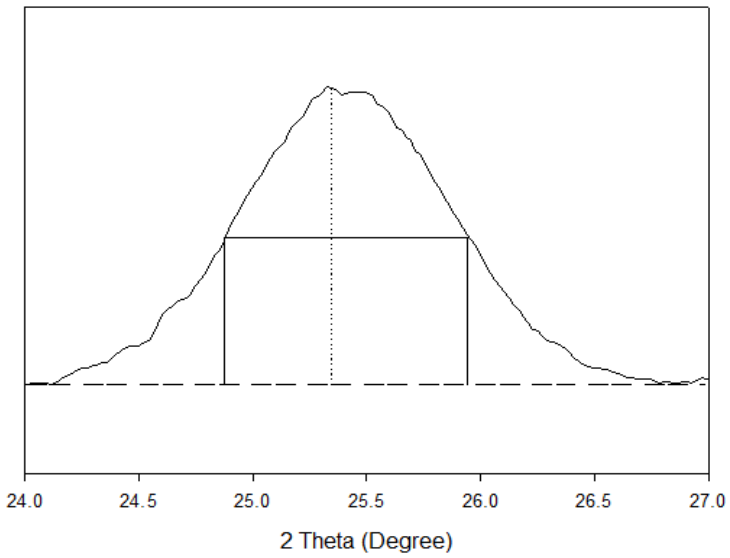

Figure A.1 The (101) diffraction peak of TiO_2 for calculation of the crystallite size

APPENDIX B

CALCULATION OF WEIGHT FRACTION OF ANATASE, RUTILE AND BROOKITE PHASE

The phase content of a sample can be calculated from the integrated intensities of peaks (2θ) at 25.32°, 27.44° and 30.88° correspond to the anatase, rutile and brookite phase, respectively.

The weight fraction of TiO_2 sample can be calculated as follows equations [30]:

$$W_A = \frac{k_A A_A}{k_A A_A + A_R + k_B A_B}$$

$$W_R = \frac{A_R}{k_A A_A + A_R + k_B A_B}$$

$$W_B = \frac{k_B A_B}{k_A A_A + A_R + k_B A_B}$$

Where

W_A = weight fraction of anatase

W_R = weight fraction of rutile

W_B = weight fraction of brookite

A_A = the intensity of the anatase peak

A_R = the intensity of the rutile peak

A_B = the intensity of the brookite peak

k_A = the coefficient factor of anatase was 0.886

k_B = the intensity factor of brookite was 2.721

Example: calculation of the phase contents of TiO_2 calcined at 400°C for two hours

Where

The intergrated intensities of anatase (A_A) = 2486

The intergrated intensities of rutile (A_R) = 984

The intergrated intensities of anatase (A_B) = 548

The weight fraction of the phase content can be calculated by as follows:

$$W_A = \frac{0.866(2486)}{0.866(24866) + 984 + 2.721(548)} = 0.47$$

$$W_R = \frac{984}{0.866(24866) + 984 + 2.721(548)} = 0.21$$

$$W_B = \frac{2.721(548)}{0.866(24866) + 984 + 2.721(548)} = 0.32$$

APPENDIX C

DETERMINATION OF THE AMOUNT OF DYE ADSORBED ON TITANIA SURFACE

The amount of dye adsorbed was determined by UV-Visible Absorption Spectroscopy. The dye was dissolved out to surface by using a mixed solution of 0.1 M NaOH and ethanol at volume ration 1:1.

The calibration curve of the concentration of dye with absorbance was illustrated in the following figure.

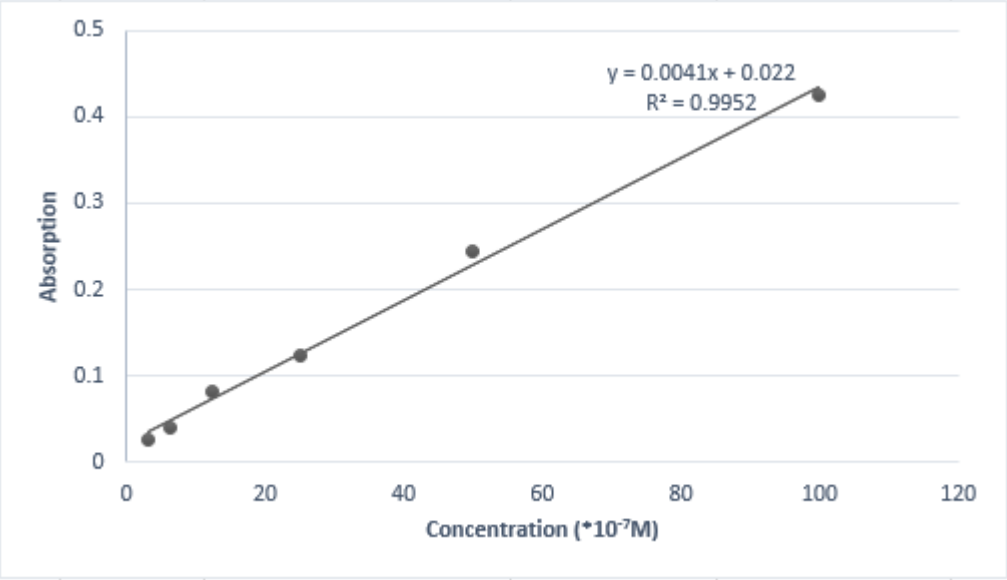

Figure C.1 The calibration curve of the concentration of N3 adsorbed dye

APPENDIX D

THE CALCULATION OF THE BAND GAP FROM UV-VIS SPECTRA

The band gap (E_g) of the sample was determined by the following equation:

$$E_g = \frac{hC}{\lambda} \qquad \text{(C.1)}$$

Where E_g is a band gap (eV)

h = Planks constant = 6.62×10^{-34} Joules sec

C = Speed of light = 3.0×10^{8} meter/sec

λ = Cut off wavelength (meters)

1 eV = 1.6×10^{-19} Joules (conversion factor)

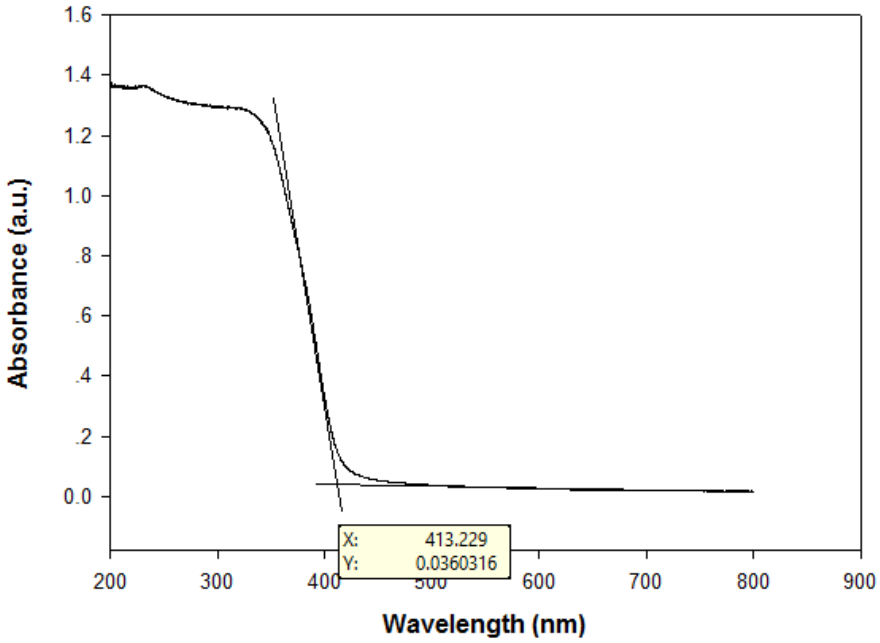

Figure D.1 UV-visible absorption characteristics of titanium dioxide

The spectra data recorded showed the strong cut off at 415 nm; where the absorbance value is a minimum.

Calculation:

$$E_g = \frac{hC}{\lambda}$$

$$E_g = \frac{(6.63 \times 10^{-34} Joules.\text{sec})(3.0 \times 10^{8}\ meter/sec)}{(413 \times 10^{-9}\ meters)(1.6 \times 10^{-19}\ Joules)} = 3.0\ eV$$

APPENDIX E

CALCULATION OF RESULT OF ICP-OES

Calculation of ICP-OES results

The results from ICP-OES characterization were calculation the contents of metal in catalysts. The example of calculation is as following:

Example: calculation of the contents of 1.0 wt% of La_2O_3/TiO_2.

For 1.0 wt% of La_2O_3/TiO_2, the initial weight of powder was 0.0340 g. Hence, the calculation of lanthanum contents as follows:

The amount of lanthanum in catalyst were;

In 100 g of the La_2O_3/TiO_2, had a La_2O_3 content was 1.0%

In 0.0340 g of the La_2O_3/TiO_2, had a La_2O_3 content was $\frac{0.0340 \times 1.0}{100}$

= 0.34 mg

For digestion, samples were diluted to 50 cm^3

Therefore;

The sample had a concentration were = $\frac{0.34 \times 1000}{50}$ = 6.8 ppm of La_2O_3

From the result of ICP-OES, shown the contents of lanthanum 5.017 ppm

Converting to a concentration of La_2O_3 = $\frac{5.017 \times 325.81}{138.91 \times 2}$ = 5.8836 ppm

Therefore;

The La_2O_3/TiO_2 contents in the catalysts were calculated by

The lanthanum trioxide concentration of 6.8 ppm refer to 1.0 % La_2O_3/TiO_2 in catalyst.

The lanthanum trioxide concentration of 5.8836 ppm refer to $\frac{5.8836 \times 1.0}{6.8}$

= 0.865 wt% of La_2O_3/TiO_2

APPENDIX F

THE ELECTROCHEMICAL PROPERTIES OF DYE-SENSITIZED SOLAR CELL

The electrochemical properties of dye-sensitized solar cell as a thickness and sintering temperature of Pure TiO_2, La_2O_3/TiO_2, Er_2O_3/TiO_2, and AgO/TiO_2 electrode by I-V tester. In this study, three samples were used, and the efficiency of cell given is the average value follow by the standard derivation.

Table F.1 Electrochemical properties of dye-sensitized solar cell of TiO_2 electrode calcined at 400°C for 2 hours 500 coats

Number of cell	V_{oc} (volt)	J_{sc} (mA·cm^{-2})	Fill factor	Efficiency (%)
1	0.68	7.02	0.73	3.48
2	0.68	6.83	0.80	3.72
3	0.66	6.79	0.74	3.32
Average	0.67	6.88	0.76	3.51±0.20

Table F.2 Electrochemical properties of dye-sensitized solar cell of 1.0%wt of La_2O_3/TiO_2 electrode calcined at 400°C for 2 hours 500 coats

Number of cell	V_{oc} (volt)	J_{sc} (mA·cm^{-2})	Fill factor	Efficiency (%)
1	0.73	6.94	0.78	3.95
2	0.72	7.22	0.73	3.79
3	0.74	6.33	0.89	4.19
Average	0.73	6.83	0.80	3.97±0.19

Table F.3 Electrochemical properties of dye-sensitized solar cell of 3.0%wt of La_2O_3/TiO_2 electrode calcined at 400°C for 2 hours 500 coats

Number of cell	V_{oc} (volt)	J_{sc} (mA·cm^{-2})	Fill factor	Efficiency (%)
1	0.74	7.80	0.84	4.85
2	0.68	6.89	0.87	4.08
3	0.73	7.21	0.86	4.52
Average	0.72	7.30	0.86	4.48±0.39

Table F.4 Electrochemical properties of dye-sensitized solar cell of 5.0%wt of La_2O_3/TiO_2 electrode calcined at 400°C for 2 hours 500 coats

Number of cell	V_{oc} (volt)	J_{sc} (mA·cm^{-2})	Fill factor	Efficiency (%)
1	0.71	7.75	0.87	4.85
2	0.76	8.26	0.87	4.08
3	0.74	7.91	0.84	4.52
Average	0.74	7.97	0.86	5.06±0.36

Table F.5 Electrochemical properties of dye-sensitized solar cell of 7.0%wt of La_2O_3/TiO_2 electrode calcined at 400°C for 2 hours 500 coats

Number of cell	V_{oc} (volt)	J_{sc} (mA·cm^{-2})	Fill factor	Efficiency (%)
1	0.70	7.44	0.67	3.49
2	0.72	7.66	0.86	4.74
3	0.74	7.05	0.82	4.28
Average	0.72	7.38	0.78	4.17±0.46

Table F.6 Electrochemical properties of dye-sensitized solar cell of 1.0%wt of Er_2O_3/TiO_2 electrode calcined at 400°C for 2 hours 500 coats

Number of cell	V_{oc} (volt)	J_{sc} (mA·cm^{-2})	Fill factor	Efficiency (%)
1	0.69	6.64	0.78	3.57
2	0.72	6.80	0.77	3.77
3	0.72	6.57	0.79	3.72
Average	0.71	6.67	0.78	3.69±0.11

Table F.7 Electrochemical properties of dye-sensitized solar cell of 3.0%wt of Er_2O_3/TiO_2 electrode calcined at 400°C for 2 hours 500 coats

Number of cell	V_{oc} (volt)	J_{sc} (mA·cm^{-2})	Fill factor	Efficiency (%)
1	0.74	7.19	0.83	4.42
2	0.77	6.93	0.76	4.06
3	0.74	7.48	0.84	4.65
Average	0.75	7.20	0.81	4.37±0.30

Table F.8 Electrochemical properties of dye-sensitized solar cell of 5.0%wt of Er_2O_3/TiO_2 electrode calcined at 400°C for 2 hours 500 coats

Number of cell	V_{oc} (volt)	J_{sc} (mA·cm^{-2})	Fill factor	Efficiency (%)
1	0.74	6.91	0.81	4.14
2	0.70	7.10	0.80	3.98
3	0.73	7.42	0.81	4.39
Average	0.72	7.14	0.81	4.17±0.21

Table F.9 Electrochemical properties of dye-sensitized solar cell of 7.0%wt of Er_2O_3/TiO_2 electrode calcined at 400°C for 2 hours 500 coats

Number of cell	V_{oc} (volt)	J_{sc} (mA·cm^{-2})	Fill factor	Efficiency (%)
1	0.72	6.88	0.84	4.16
2	0.70	6.93	0.76	3.69
3	0.75	6.65	0.84	4.19
Average	0.72	6.82	0.81	4.01±0.28

Table F.10 Electrochemical properties of dye-sensitized solar cell of 1.0%wt of AgO/TiO_2 electrode calcined at 400°C for 2 hours 500 coats

Number of cell	V_{oc} (volt)	J_{sc} (mA·cm^{-2})	Fill factor	Efficiency (%)
1	0.64	5.58	0.68	2.43
2	0.61	5.83	0.71	2.52
3	0.66	5.03	0.71	2.36
Average	0.64	5.48	0.70	2.44±0.08

Table F.11 Electrochemical properties of dye-sensitized solar cell of 3.0%wt of AgO/TiO_2 electrode calcined at 400°C for 2 hours 500 coats

Number of cell	V_{oc} (volt)	J_{sc} (mA·cm^{-2})	Fill factor	Efficiency (%)
1	0.66	3.38	0.68	1.52
2	0.70	4.22	0.60	1.77
Average	0.68	3.80	0.64	1.64±0.18

Table F.12 Electrochemical properties of dye-sensitized solar cell of 5.0%wt of AgO/TiO_2 electrode calcined at 400°C for 2 hours 500 coats

Number of cell	V_{oc} (volt)	J_{sc} (mA·cm^{-2})	Fill factor	Efficiency (%)
1	0.62	1.84	0.60	0.68
2	0.60	2.22	0.66	0.88
Average	0.61	2.03	0.63	0.78±0.14

Table F.13 Electrochemical properties of dye-sensitized solar cell of 5.0%wt of AgO/TiO_2 electrode calcined at 400°C for 2 hours 500 coats

Number of cell	V_{oc} (volt)	J_{sc} (mA·cm^{-2})	Fill factor	Efficiency (%)
1	0.62	0.49	0.60	0.18
2	0.58	0.66	0.53	0.20
3	0.61	0.69	0.63	0.27
Average	0.60	0.61	0.59	0.22±0.04

Table F.14 Electrochemical properties of dye-sensitized solar cell of double-layered electrode of 5% La_2O_3/TiO_2 and Pure TiO_2 calcined at 400°C for 2 hours 500 coats

Number of cell	V_{oc} (volt)	J_{sc} (mA·cm^{-2})	Fill factor	Efficiency (%)
1	0.70	12.73	0.88	7.84
2	0.69	14.16	0.83	8.11
3	0.72	12.49	0.80	7.19
Average	0.70	13.13	0.84	7.72±0.47

VITA

Mr. Tanya Jakawanorasing was born on December 21, 1990 in Rayong province, Thailand. He finished high school from Rayongwittayakon school, Thailand, and received the bacherlor's degree of Chemical Engineering, King Mongkut's University of Technology Thonburi, in 2012. He continued his master degree in Chemical Engineering at Chulalongkorn University.

Tanya Jakawanorasing and Akawat sirisuk. Dye sensitized solar cells with TiO2 electrode modified by La2O3, Er2O3 or AgO. Proceeding of pure and applied chemistry international conference, Amari Watergate Hotel, Bangkok, Thailand. Jan. 21-23, 2015 (PACCON2015)